Defence Technology 43 (2025) 225–251

Contents lists available at ScienceDirect

Defence Technology

journal homepage: www.keaipublishing.com/en/journals/defence-technology

Perspectives on additive manufacturing for warhead applications

Hao Xue [a], Qiang Zhou [b], Chuan Xiao [b, **], Guangyan Huang [a, c, *]

[a] State Key Laboratory of Explosion Science and Technology, Beijing Institute of Technology, Beijing 100081, China
[b] Ordnance Science and Research Academy of China, Beijing 100089, China
[c] Beijing Institute of Technology Chongqing Innovation Center, Chongqing 401120, China

ARTICLE INFO

Article history:
Received 16 July 2023
Received in revised form
11 January 2024
Accepted 27 February 2024
Available online 19 March 2024

Keywords:
Additive manufacturing
Fragmentation warhead
Shaped charge warhead
Penetrating warhead
Warhead charge

ABSTRACT

According to different damage modes, warheads are roughly divided into three types: fragmentation warheads, shaped charge warheads, and penetrating warheads. Due to limitations in material and structural manufacturing, traditional manufacturing methods make it difficult to fully utilize the damage ability of the warhead. Additive manufacturing (AM) technology can fabricate complex structures, with classified materials composition and customized components, while achieving low cost, high accuracy, and rapid production of the parts. The maturity of AM technology has brought about a new round of revolution in the field of warheads. In this paper, we first review the principles, classifications, and characteristics of different AM technologies. The development trends of AM technologies are pointed out, including multi-material AM technology, hybrid AM technology, and smart AM technology. From our survey, PBF, DED, and EBM technologies are mainly used to manufacture warhead damage elements. FDM and DIW technologies are mainly used to manufacture warhead charges. Then, the research on the application of AM technology in three types of warhead and warhead charges was reviewed and the existing problems and progress of AM technologies in each warhead were analyzed. Finally, we summarized the typical applications and look forward to the application prospects of AM technology in the field of warheads.

1. Introduction

The warhead is a key component in destroying targets, which plays a "one step at the door" role in the weapon system. According to types of warhead damage elements, the warhead can be generally divided into fragmentation, shaped charge, and penetrating warheads. The main structures and damage mechanisms of the three types of warheads are shown in Fig. 1. The main structures of the warhead include the shell, the charge, the detonation and safety device, and so on. A large number of high-speed fragments are formed to attack armored vehicles and personnel targets under the explosion of high-energy explosives in the fragmentation warhead, in which the fragments are the main damage elements [1]. The shaped charge warhead is used to attack armored tank and vehicle targets, relying on a concentrated and high-speed metal jet that appears on the axis of the warhead after the explosion of the grooved explosive. The metal jet striking the target is the main damage element [2]. The penetrating warhead has usually a thick shell (high penetration ability) and massive charge (high blast effect), and the concrete plate is its main target. The penetrating warhead strikes the target relying on the dual effects of penetration ability and explosion effect.

The traditional manufacturing processes of fabricating warheads include turning, milling, drilling, grinding, cutting, and boring methods, most of which belong to the "subtractive manufacturing" (SM) process as the product is fabricated by removing materials. The materials used in the SM process have stable mechanical properties, and the research on the lethality characteristics of the traditional warhead structures fabricated by SM is relatively mature. However, SM often faces the problems of cumbersome manufacturing steps, low material utilization, and large manpower consumption. The emergence and increasing maturity of additive manufacturing (AM) technology have brought innovations to the field of warheads. From a patent on light curing

* Corresponding author.
** Corresponding author.
E-mail addresses: xchuan2022@163.com (C. Xiao), huanggy@bit.edu.cn (G. Huang).
Peer review under responsibility of China Ordnance Society

https://doi.org/10.1016/j.dt.2024.02.010

Acronym meaning

AM	Additive Manufacturing
SM	Subtractive Manufacturing
ASTM	American Society for Testing and Materials
MMAM	Multi-Material Additive Manufacturing
TO	Topology Optimization
DED	Directed Energy Deposition
PBF	Powder Bed Fusion
FDM	Fused Deposition Modeling
DIW	Direct Ink Writing
ME	Material Extrusion
MJ	Material Jetting
VP	Vat Polymerisation
SL	Sheet Lamination
SLM	Selective Laser Melting
BJ	Binder Jetting
EBM	Electron Beam Melting
DMLS	Direct Metal Laser Sintering
SLS	Selective Laser Sintering
LMD	Laser Melting Deposition
UV	Ultraviol
LOM	Laminated Object Modeling
SRM	Structural Reactive Material
BCC	Body-Centered Cubic
SS316L	316L Stainless Steel
TPMS	Three Period Minimum Surface
WHAs	Tungsten Heavy Alloys
BMGs	Bulk Metallic Glasses
HEAs	High Entropy Alloys
SEM	Scanning Electron Microscope
EBSD	Electron Backscatter Diffraction
XRD	X-Ray Diffraction
DSC	Differential Scanning Calorimetry
WPU	Waterborne Polyurethane
EC	Ethyl Cellulose
EFP	Explosively Formed Penetrator
MEFP	Multiple Explosively Formed Penetrator
DBTT	Ductile-to-Brittle Transition Temperature
RMS	Reactive Material Structure

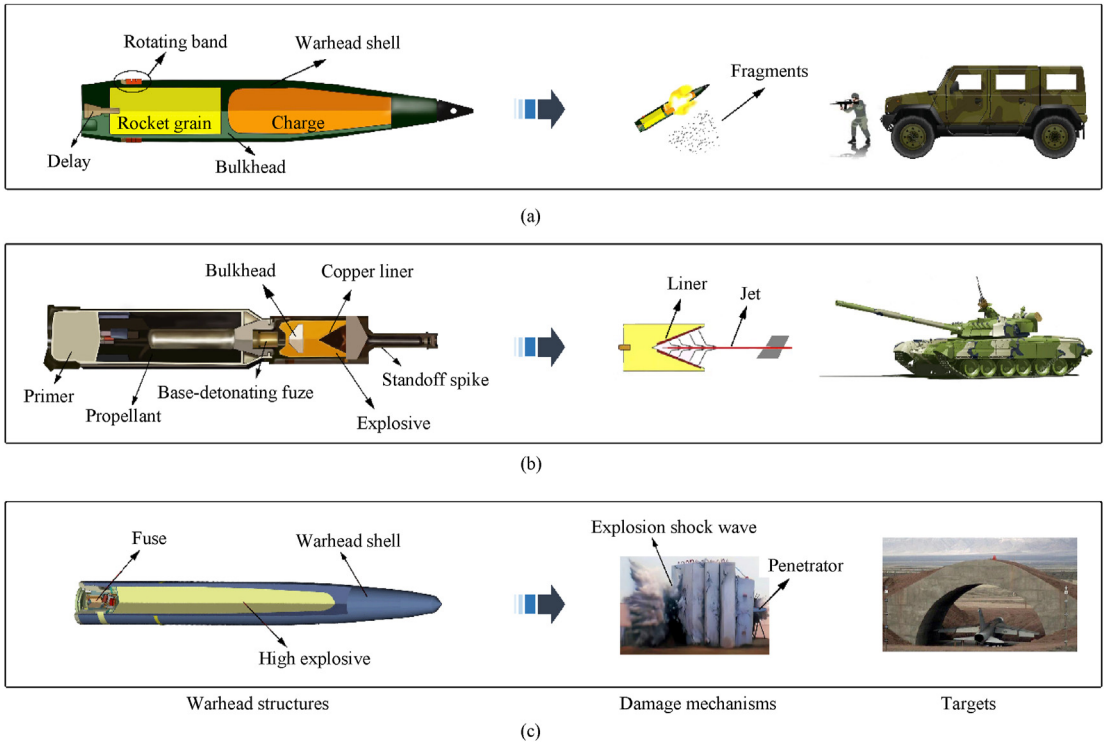

Fig. 1. The main structures of three types of warheads and their damage mechanisms to typical targets: (a) Fragmentation warheads; (b) Shaped charge warheads; (c) Penetrating warheads.

technology by Hull in 1986, it was not until 2002 that Germany took the lead in developing the Selective Laser Melting (SLM) equipment [3]. After more than 30 years of development, AM technology has ushered in unprecedented prosperity. AM is described as "a technology in which the initial model generated by a three-dimensional computer-aided design system can be directly manufactured without process planning", that is, "thin-layer printing, layer-by-layer overlay" [4]. Compared to the SM process, AM technology is capable of manufacturing complex structures, and customizing products with specific functions and high precision. Moreover, AM technology has significant advantages in improving component production efficiency. It does not require any molds during the manufacturing process, which greatly simplifies the process steps [5]. These advantages of AM technology provide more possibilities for improving the lethality characteristics of warheads. For instance, the special-shaped warhead damage element and charge structures are expected to change the power distribution of the warhead and thereby enhance the attack capability. It is reported

that AM technology has been used to manufacture warheads [6–8].

The author's team initially carried out exploratory research on the application of AM technology in small-caliber bullets. In the ballistic test between the 316L AM projectile and traditional projectiles, the ballistic performance of the AM projectile was about 8% weaker than that of traditional projectiles, demonstrating the penetration potential of AM materials [9]. Furthermore, we completed the structural design and AM of a lightweight projectile based on topology optimization (TO) theory and the Concept M2 printer and compared the penetration performance of AM solid projectiles and topological projectiles. The weight of topological projectiles is about 30% less than that of solid projectiles. In the comparison of ballistic performance results based on the specific kinetic energy method, the ballistic performance of topological projectiles is equivalent to that of solid projectiles [10]. Although this is a simple application study of TO combined with AM, it provides a foundation for the engineering design and application of large-scale AM penetrating warheads. In subsection 3.3, we will also review the research of the U.S. Air Force Institute of Technology on using AM and TO methods to manufacture penetrating warheads. In fact, given the performance potential of AM materials, coupled with its unique advantages in manufacturing complex structures, the idea of TO combined with AM for warhead design can be continuously improved. So far, no one has tried to integrate AM functions into TO algorithms from the software level, and there is no case of tightly integrating AM equipment and TO design modules from the hardware level. This is still a very open research field. Not limited to this, the relevant research on the application of AM technology in typical warheads needs to be reviewed urgently to clarify the current status, technical problems, and development direction of the AM technologies applied in the fields of warheads.

In this review, the principles and characteristics of different AM technologies are first introduced. The development direction of new AM technologies was pointed out, including multi-material AM (MMAM) technology, hybrid AM technology, and smart AM technology. In the warhead field, Powder Bed Fusion (PBF), Directed Energy Deposition (DED), and Electron Beam Melting (EBM) are the main technologies to manufacture warhead damage elements. Fuse Deposition Modeling (FDM) and Direct Ink Writing (DIW) technologies are mainly used to manufacture the warhead charge. Then the research status of the application of AM technology on fragmentation warheads, shaped charge warheads, and penetrating warheads is systematically elaborated. The research progress of AM warhead charges is also reviewed from two aspects: new high-energy and insensitive explosives and high-precision and energy-customized explosives. Finally, we summarized the application progress of AM technology in warhead damage elements and charges and prospected the development of AM technology in warhead fields.

2. Principles and characteristics of AM technology

2.1. Basic principles of AM technology

According to ISO/ASTM 52900, AM technology is divided into seven categories: Binder Jetting (BJ), DED, PBF, Material Extrusion (ME), Material Jetting (MJ), Vat Polymerisation (VP), and Sheet Lamination (SL) [4]. Their basic principles are as follows.

- Binder Jetting (BJ)

BJ technology selectively prints the binders on the powder bed to join the powders layer-by-layer to form a green part, as shown in Fig. 2(a). First, a roller is used to spread the powder material on a platform, and then the print head deposits a binder on top of the powder, which combines with the binder to form a solid layer. Finally, the platform is gradually lowered based on the layer thickness and a new layer of powder is laid on top of the previous layer. This process is repeated to form the final object. It should be noted that objects printed by the BJ method often need to be degreased and sintered to increase their density and strength. Since no heat source is introduced during the BJ process, BJ is suitable for manufacturing most materials such as metals, polymers, and ceramics. The printing process is also relatively faster because more nozzles can be added. However, the use of binders makes the BJ method not always suitable for structural parts, and post-processing operations such as sintering will significantly increase the manufacturing time of the product [11].

- Powder Bed Fusion (PBF)

PBF technology usually uses a high-energy laser to selectively melt specific areas of a powder bed such as metal, ceramic, or polymer layer by layer to form a 3D model, which is the most important technology for manufacturing warhead damage elements. The principle diagram of the PBF is shown in Fig. 2(b). The main PBF technologies include SLM, Direct Metal Laser Sintering (DMLS), and Selective Laser Sintering (SLS).

SLM technology can efficiently achieve complex shapes or internal features. Many metals (titanium alloy, aluminum alloy, cobalt-chromium alloy stainless steel (SS), etc.) can be manufactured by SLM and the final parts have the same performance as traditional manufacturing processes. However, SLM also has disadvantages such as high cost and extensive post-processing. The principle of DMLS technology is the same as that of SLM. Two terms are usually used interchangeably. SLS technology usually uses laser-sintered polymer powder materials (typically polyamide). The main difference between SLS and SLM technology is the raw materials. SLS mainly uses nylon (PA) polymer materials, and SLM is specifically used for metals. In addition, due to the limitations of the SLM process and the material weight, SLM requires the addition of support structures to any overhanging positions, whereas the SLS can form parts with free shapes without adding supports.

- Directed Energy Deposition (DED)

DED technology describes the process in which the energy source (laser or electron beam) and material (in the form of powder or filament) are simultaneously sent to the high-temperature melting zone and the latter is deposited layer by layer to form the product, whose schematic is presented in Fig. 2(c). Specially, when laser is used as the energy source and metal powder is used as the raw material, it is also called LMD technology. The characteristics of LMD technology are introduced as follows.

(1) Unlike SLM, LMD does not rely on a pressure chamber. Because the inert gas (usually argon) flows directly from the laser head and surrounds the powder flow and melt pool, the 3D printing process can start immediately. In contrast, the pressure chamber must be filled with inert gas before SLM printing.
(2) LMD does not require any support structures, which offers significant advantages over powder bed methods.
(3) Compared with SLM, LMD has a relatively slow cooling rate and a larger melt pool, resulting in different substructures, especially element-enriched zones at cell boundaries [20].

Besides, LMD allows the laser head and parts to move more flexibly and accurately deposit materials anywhere in the build chamber, which provides the possibility to increase design freedom

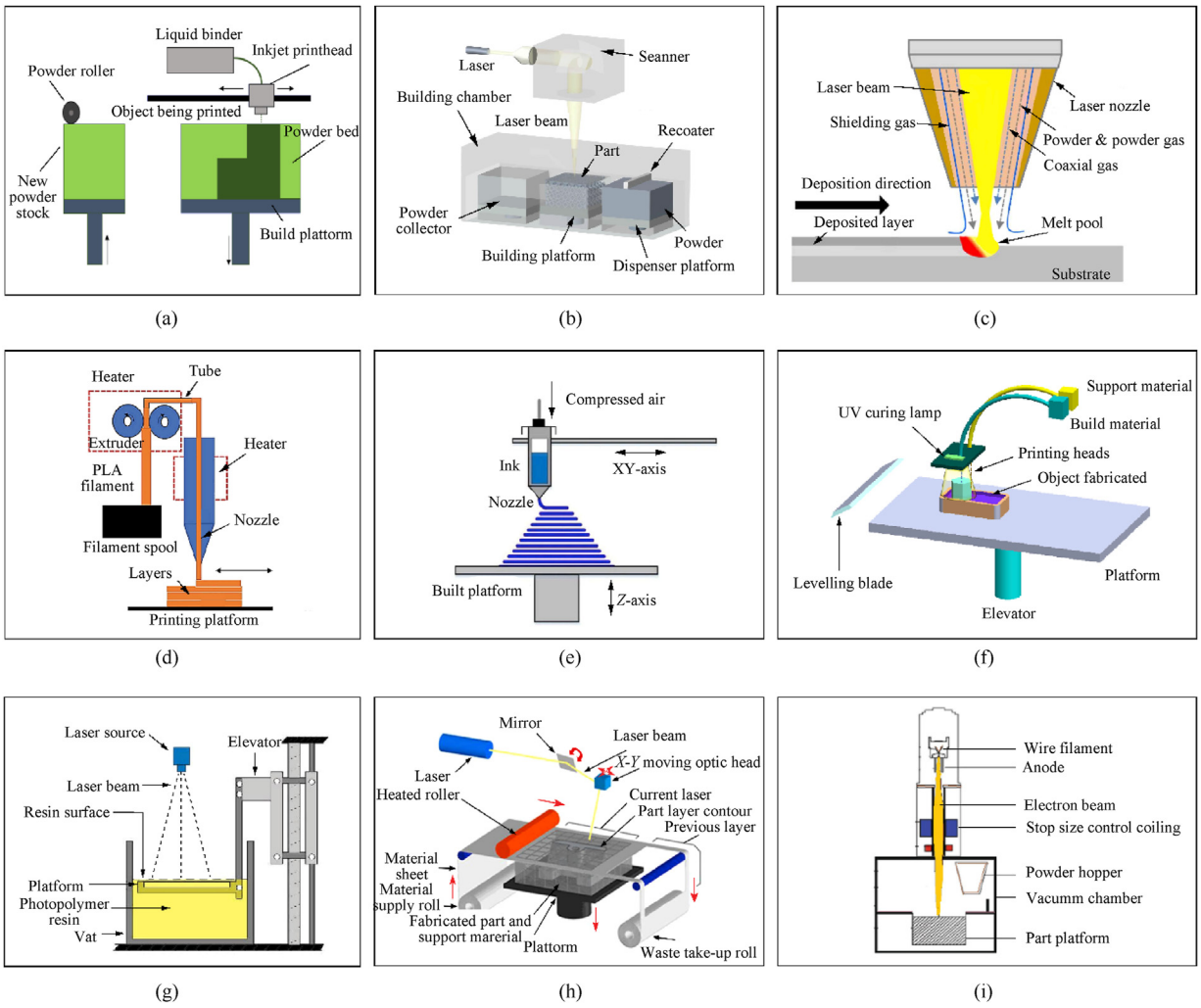

Fig. 2. The principle diagram of different AM technologies: (a) BJ technology (adapted from Ref. [11]); (b) PBF technology (adapted from Ref. [12]); (c) DED technology (alternatively LMD, adapted from Ref. [13]); (d) FDM technology (adapted from Ref. [14]); (e) DIW technology (adapted from Ref. [15]); (f) MJ technology (adapted from Ref. [16]); (g) VP technology (adapted from Ref. [17]); (h) SL technology (adapted from Ref. [18]); (i) EBM technology (adapted from Ref. [19]).

and quickly manufacture large parts. However, the LMD process is not as precise as SLM and often requires more post-processing to obtain parts that meet the requirements.

- Material Extrusion (ME)

As the name suggests, ME technology produces parts by extruding materials through a heated nozzle. FDM is the most common ME process. During the FDM process, thermoplastic filaments are continuously extruded through a heated nozzle, and the extruded filaments are stacked layer by layer on the building platform to achieve high-temperature melt printing of thermoplastic polymer materials [14]. The principle diagrams of FDM are illustrated in Fig. 2(d). During the layer-by-layer manufacturing process, residual stress will accumulate, which will lead to warping deformation and inter-layer delamination of the parts, seriously affecting the accuracy and mechanical properties of the parts.

DIW technology is extended from automatic grouting technology and is mainly divided into high-viscosity slurry direct writing and droplet-based inkjet printing. By controlling the shape of the ink after being accumulated layer by layer, the rheological properties of the ink are used to realize the printing and manufacturing of three-dimensional complex structures. After continuous improvement and development, DIW technology has been able to be used in the manufacture of a variety of gel and polymer materials. The principle diagrams of DIW are shown in Fig. 2(e).

Both FDM and DIW technologies have the advantages of low equipment requirements, low manufacturing costs, and a wide range of raw material applications. FDM molding speed is slow and dimensional accuracy is low, making it unsuitable for items with fine features. Although the molding accuracy of DIW is higher than that of FDM, the accuracy of the final parts not only depends on the formula of the ink material, the physical and chemical properties of the parts, system viscosity, rheological properties but is affected by direct writing parameters (nozzle diameter, pressure, platform movement speed, etc.) [21].

- Material Jetting (MJ)

MJ technology is a process of building three-dimensional objects using a moving inkjet nozzle. It directly injects photopolymer into the platform in the form of droplets, which solidify and build the model layer by layer. Fig. 2(f) shows a schematic of the MJ process. Because materials must be deposited in the form of droplets, the materials available for MJ are limited, and polymers are the most suitable and commonly used materials. However, droplet

deposition also enables the fabrication of objects with high precision (a resolution of approximately 10–30 μm), and parts can be manufactured using a variety of materials and colors [16].

- Vat Polymerisation (VP)

VP is a process in which photoreactive polymers are cured by laser, light, or ultraviolet (UV) light. As each layer solidifies, the platform moves downward and builds more layers on top of the previous one, forming the final three-dimensional object. Because the VP process uses a liquid to form the object, no structural support is needed when the object is being built. VP's essential parameters include the exposure period, wavelength, and power source. VP can effectively produce parts with a high level of accuracy and good finish [17]. However, expense and the use of light resin materials with wires are its main disadvantages. Fig. 2(g) presents the manufacture of parts during the VP process.

- Sheet Lamination (SL)

SL technology, also known as Laminated Object Modeling (LOM), can be used to create objects by cutting, sequentially laminating, and bonding. In the SL process, metallic sheets or layers of plastic coated with adhesive are bonded together through ultrasonic welding and shaped by a laser cutter [22]. The three-dimensional object is finally built through layer-by-layer bonding. The principle schematic of SL technology can be seen in Fig. 2(h). Therefore, the strength of an object made by SL is entirely dependent on the binder used, and the materials used are entirely limited. However, SL has the advantages of high speed, low cost, and easy material handling, which makes it widely used.

2.2. New AM technologies and methods

With the development of AM technology, a series of new AM technologies and methods have gradually emerged, for example, EBM technology, multi-material AM technology, hybrid AM technology, and closed-loop intelligent melting technology, which make AM have more unique capabilities when facing structural complexity, material complexity, hierarchical complexity and functional complexity manufacturing demands [23].

- Electron beam melting (EBM)

EBM technology is a type of powder bed technology. As shown in Fig. 2(i), EBM technology uses high-energy electron beams as the energy source, the energy density of which exceeds several kilowatts. Before printing, the electron beam will quickly scan the powder layer many times to preheat it. The powder is in a slightly sintered state without being melted. This is a unique step of EBM, and the others are the same as SLM technology. In addition, EBM and SLM technologies are different in terms of molding environment, pre-heat temperature, powder thickness, and powder size, as shown in Table 1. Due to the high energy density of the electron beam, the powder melts quickly and the molding speed is very fast.

Table 1
Comparison of the differences between SLM and EBM technologies [25].

	SLM	EBM
Energy source	Laser	Electron beam
Molding environment	Inert atmosphere (Ar, N_2)	Vacuum
Pre-heat temperature/°C	Maximum 300	600–1200
Layer thickness/μm	10–100	50–200
Powder size/μm	5–53	45–105

The high energy density can melt metals with melting points as high as 3400 °C, which is a good choice for printing the refractory tungsten alloys commonly used in penetrating warheads. Moreover, the preheating of each layer of powder by the electron beam can greatly reduce the residual stress of the parts and improve the quality of the parts. In a word, the main feature of the EBM process is the rapid production of complex structural parts with mechanical properties similar to those of heat-treated materials [24]. However, EBM also has some shortcomings, such as more expensive equipment and rougher surface quality than SLM technology.

- Multi-material AM (MMAM) technology

The specific distribution of multiple materials in a component can achieve better performance than a single material component. MMAM technology is an AM technology that prints multiple materials at the same time, which brings opportunities to achieve high personalization and functionality of products. Typical MMAM material combination types include metal/metal, metal/ceramic, metal/glass, and metal/polymer. Regardless of the material combination, achieving a void- and crack-free interface and achieving a strong bond is most critical. So far, MMAM technology is still in its infancy, and there are still a series of technical issues in interface strengthening methods, equipment development, thermodynamic calculations, and powder cross-contamination [26]. But there are also some gratifying developments, such as Kraken, the world's largest multi-material hybrid AM system, which can deposit and manufacture two types of materials (metal and resin) at the same time [27]. What's important is that Kraken has reached marketization conditions. MMAM technology will have good application prospects in warheads. For the penetrating warhead, the requirements for warhead materials are different when penetrating to different depths. Thus a penetrating warhead with gradient materials may be a new attempt.

- Hybrid AM technology

From the several AM technologies introduced in subsection 2.1, it can be found that directly formed parts often require appropriate machining post-processing to meet engineering needs. Therefore, a better solution should be proposed to make the manufacturing of parts more precise and efficient. Hybrid AM technology is the solution to this need, the purpose of which is to combine the advantages of AM and SM and minimize the disadvantages of the two manufacturing methods. Hybrid AM technology has made some progress since the concept was proposed, especially in commercial machines. The LASERTEC 65 3D Hybrid was presented by DMG Mori In 2014, which can build pieces inscribed in a cylindrical space with a base of 600 mm and a weight of 600 kg [28]. Ibarmia presented the ZVH 45/1600 machine in 2015, that integrates LMD with CNC milling and turning [29]. The OPM series was developed by Sodick in 2017 and combines SLM and high-speed CNC milling [28]. The advantages of the hybrid AM process have been demonstrated, and existing research shows that the efficiency of the hybrid AM process is significantly higher than that of a single CNC machining manufacturing process. Of course, the future trend is not just to simply combine AM and SM processes on the same platform, but also to incorporate intelligent sensing technology into hybrid AM systems, moving towards all-round intelligent manufacturing [30].

- Smart AM technology

Smart AM refers to a fully integrated, collaborative AM system that responds in real-time to support ubiquitous intelligent design, manufacturing, and service of 3D printed products [31]. Although

AM technology has obvious advantages over traditional manufacturing methods, with the promotion and application of AM technology, printing quality problems caused by defects such as excessive melting and lack of fusion have begun to appear. One of the fundamental reasons is that the printing parameters remain unchanged during the printing process and cannot adapt to minor fluctuations in the environment during the printing process. Therefore, related research on real-time monitoring and closed-loop control of laser power, temperature, etc. during the printing process began to develop. For example, EOS launched Smart Fusion (closed-loop intelligent fusion technology) in 2023 [32]. Smart Fusion can automatically adjust laser power by measuring the laser energy absorbed by the powder bed, effectively solving potential manufacturing problems. By constantly monitoring the welding process and collecting real-time data, Smart Fusion can identify and optimize areas of energy input, reducing defects and enhancing the overall performance of the part. At the same time, Smart Fusion can also detect and correct deviations such as powder particle size distribution, process abnormalities, and powder splash in real time to achieve high-quality printing. Therefore, intelligent AM systems are the future development trend of AM technology.

2.3. AM technology in warhead manufacturing

According to the characteristics of the above-mentioned AM technology and the material properties of the warhead damage element and charges, the common AM technologies used for warhead damage elements and charges are summarized in Fig. 3. Since the warhead damage elements are usually made of metal and the warhead charges are generally the polymers, PBF, DED, and EBM are the main technologies to manufacture warhead damage elements, while FDM and DIW technologies are the main technology for the warhead charge.

3. Application of AM in warhead damage element

The proportion of typical studies on the application of AM technology in the field of warheads is illustrated in Fig. 4. The total number of publications on the application of AM technology in the field of warheads is 48. We can find that AM technology has been studied more in fragmentation warheads and penetration warheads, accounting for 27.1% and 22.9% respectively. Among fragmentation warheads, the controlled fragment is the mainstay, accounting for 14.6%. These statistical results roughly provide a glimpse into the main warhead application types of AM technology. In addition, we also summarized the main AM materials used in warhead damage elements. The number of publications using steel materials (SS316L, 15-5 precipitation hardening (PH) SS, etc.) is 21, accounting for 70%. The tensile properties of AM SS316L and 15-5 PH are comparable with the traditional version [33–35], as illustrated in Table 2. Three publications on the application of copper alloys (CuSn10 alloy) mainly used in shaped charge warheads. Applications of other AM materials are currently still scarce.

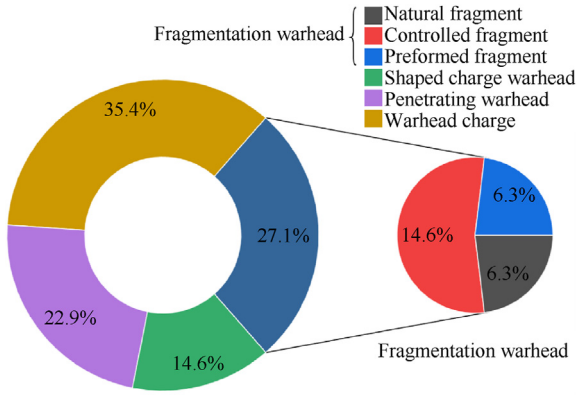

Fig. 4. Proportion of typical studies on the application of AM technology in the field of warheads.

3.1. Fragmentation warhead

The fragmentation warhead is mainly divided into natural fragment, controlled fragment, and preformed fragment warheads, and its core is to maximize the power effect by adjusting the material and structure of the damaged element and the matching relationship between fragments and charges. Generally speaking, indicators of effective killing capability include fragment velocity, fragment mass, fragment scattering density, fragment energy release, and fragment dispersion angle. The advantages of AM technology in manufacturing complex structures enable it to further improve the structural designability of the fragmentation warhead. AM technology increases the development opportunities for fragmentation warheads. While improving the above-mentioned lethality indicators, it can also greatly improve the manufacturing efficiency of the warhead. It is reported that a lethality-enhanced munition (LEO) warhead is used on a hypersonic aircraft of the US Orbital ATK Company [39]. The warhead has a special-shaped structure, and three of the five components are manufactured using AM technology. The manufacturing cycle has saved at least one and a half months compared to traditional processes.

Thirteen publications on the application of AM technology in fragmentation warheads can be found. For natural fragmentation warheads, new AM materials can better change the fragmentation of the natural shell, increasing the fragment scattering density and the killing capability of the warhead. For the controlled fragmentation warhead, shell grooves are its main form [40]. However, it is difficult to manufacture complex grooves with specific depths using traditional methods [41]. AM technology can efficiently manufacture different forms of shell grooves, thereby better controlling the fragment mass and scattering density and achieving a controllable fragmentation-killing effect. For the preformed fragment warheads, inert metals (steel and tungsten alloys, etc) are chosen as the main materials. Given the gradual trend of reactive

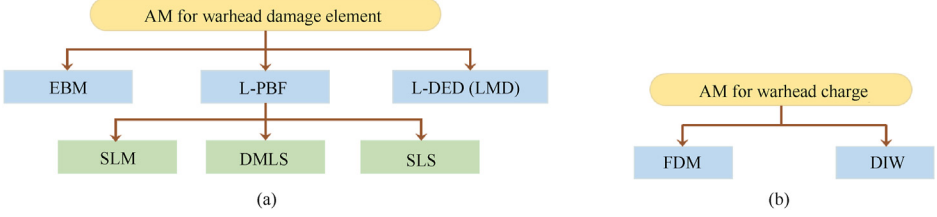

Fig. 3. AM technology for warhead manufacturing: (a) AM for warhead damage element; (b) AM for warhead charge.

Table 2
Comparison of mechanical properties of AM and traditional manufacturing SS316L, 15-5 PH, and CuSn10 materials.

Material	Printing direction	Yield strength/MPa	Tensile strength/MPa	Strain at break/%	Ref.
SLM SS316L	Horizontal	570	720	48	[36]
	Vertical	510	610	18	
Reference (wrought)	–	346	651	47	[37]
SLM 15-5 PH	Horizontal	1297	1450	12.53	[34]
	Vertical	1100	1467	14.92	
Reference (wrought)	–	1170	1310	–	
SLM CuSn10	–	399	490	19	[38]
Reference (casting)	–	360	170	6	

Note: '–' means that the corresponding data is not obtained.

fragments (such as Al/PTFE, W/PTFE, and W/PTFE/Al) replacing inert fragments [42–45], AM reactive materials can greatly enhance the energy-release effect of fragments. In short, AM technology has specific application advantages in different fragmentation warheads and has the potential to change the damage capabilities of the warhead.

3.1.1. Natural fragments

Natural fragments are formed through the rupture of the shells under the internal explosive loads. Natural shells are usually made of steel, such as 50SiMnVB steel, ANSI 1045 steel, 40CrMnSiB steel, etc. Now only three related studies on AM natural fragments have been reported, both of which involve the fragmentation behavior of AM steel shells. Amott et al. [46] studied the fracture properties of SLM SS316L cylinders with and without defects by an expanding cylinder experiment. Compared with the conventionally wrought cylinder, the SLM cylinder without defects failed at a 1.5 times higher strain and produced approximately 1.2 times larger fragment widths, indicating the larger ductility of the SLM cylinder. This difference in ductility was due to the preferential orientation of the grains that were generated during the AM process. From the microscopic results (Fig. 5(a)), the SLM sample is anisotropy, while the conventional sample is equiaxed. Interestingly, a customized fragmentation effect of the natural shell was achieved by introducing macroscopic defects into the AM shell, as shown in Figs. 5(b) and 5(c). LeSieur et al. [47] studied the fragmentation characteristics of explosion-driven DMLS 15-5 PH SS cylinders. The deformation and fragmentation behavior of the DMLS and traditional 15-5 PH SS cylinders with an outer diameter of 0.737 cm was compared and the explosion images at 6.0 μs and 33.0 μs are shown in Figs. 5(d) and 5(e). DMLS cylinders can endure explosive loadings, while DMLS cylinder has a relatively smaller shell expansion and fragmentation performance in comparison to the machined cylinder, which may be due to the microstructural formations and defects during the DMLS process. Callahan et al. [48] studied the crushing performance of AM SS316L spherical shell sections under explosion loading. The average crushing toughness value of the AM SS316L spherical shell was calculated to be 174 MPa/m$^{1/2}$ by using an energy balance method, which is equivalent to the results of forging SS304 tested under similar conditions. However, the average tensile failure strain is 0.27, which is significantly lower than the 0.38 of forged SS304. The reduction in failure strain is attributed to the early failure of the surface grooves of the 316L spherical shell under high-stress conditions. Although relevant studies are still rare, AM appears to be a reasonable manufacturing method for high-strain rate applications.

3.1.2. Controlled fragments

Gousman et al. [49] first envisioned fabricating warhead structures by using direct manufacturing technologies, including an integral shell having regions of controlled and varied structural parameters in additively deposited, direct-manufactured layers. Before the emergence of SLM technology, high-energy beam processing technologies (such as laser remelting and surface modification) were mainly used to fabricate controlled shells. Li et al. [50] studied the fragmentation angle, density, and perforation rate of high-energy beam projectiles. The fragmentation angle of the projectile at 3 m was less than 18° and the penetration rate of the 2 mm thick Q235 steel plate at 3 m was 80%, indicating a good fragmentation control effect. Villano et al. [51] compared the application performance of four processing methods (laser deep melting, laser drilling, chemical nitriding, and double casings) to maximize the control capability in the fragments' formation. The tensile strength of martensitic steel was reduced by 26% and 32% respectively after using deep laser melting and laser drilling methods, while the tensile strength of the samples using the chemical nitriding method was not changed. The impact energy of the samples obtained by the first three methods was reduced by 29%, 65%, and 28%, respectively. The reduction in tensile strength and impact energy implies that these samples are expected to achieve better crushing effects under detonation conditions. It has been verified that all the solutions performed better than the natural fragmentation reference in a detonation test. Lu et al. [52] used laser remelting technology to fabricate a certain type of rocket bullet shell grooving. The hardness of the shell surface after remelting was increased by more than 70%, which verified the feasibility of laser remelting technology for bullet shell grooving. The influence of laser parameters on the geometric characteristics and material properties of welds and grooves was also studied. Liu et al. [53] concluded that the larger the laser power, the larger the depth of the weld and groove. So the hardness of the weld region and the brittleness of the material increased significantly, which is conducive to effective control of fragmentation.

High-energy beam technologies had certain limitations in the processing of the inner surface of the shell and complex structures. SLM technology completely breaks through these limitations and makes the design and manufacturing of controlled shells more flexible. Guo et al. [54] studied the initial velocity, spatial distribution, and shell expansion radius changes of the SLM-controlled fragments made of SS316L material under different groove depths. As the groove depth increased, the shell was easier to fail, the kinetic energy of the fragments was less and the initial velocity was also smaller. However, if the groove depth is too small, the shell fragmentation will be affected. Therefore, SLM is effective in manufacturing controlled shells with suitable groove depth. It has been proved that the mass recovery rate of the fragments of the SLM-controlled shell was larger than that of the traditional shell by a crushing test. More concepts of controlled fragmentation warheads were developed by Lukas et al. [55], as illustrated in Fig. 6(a), including the reference design, conical straight line design, circular parabola design, sector convex structure, thin plate shell sector convex structure, sector concave structure, and thin plate sector concave structure. These structures change the shape of the warhead shell and concentrate the dispersion angle of the fragments after the explosion into a circular sector of less than ±20°, which helps to achieve the fragment-focusing effect of the

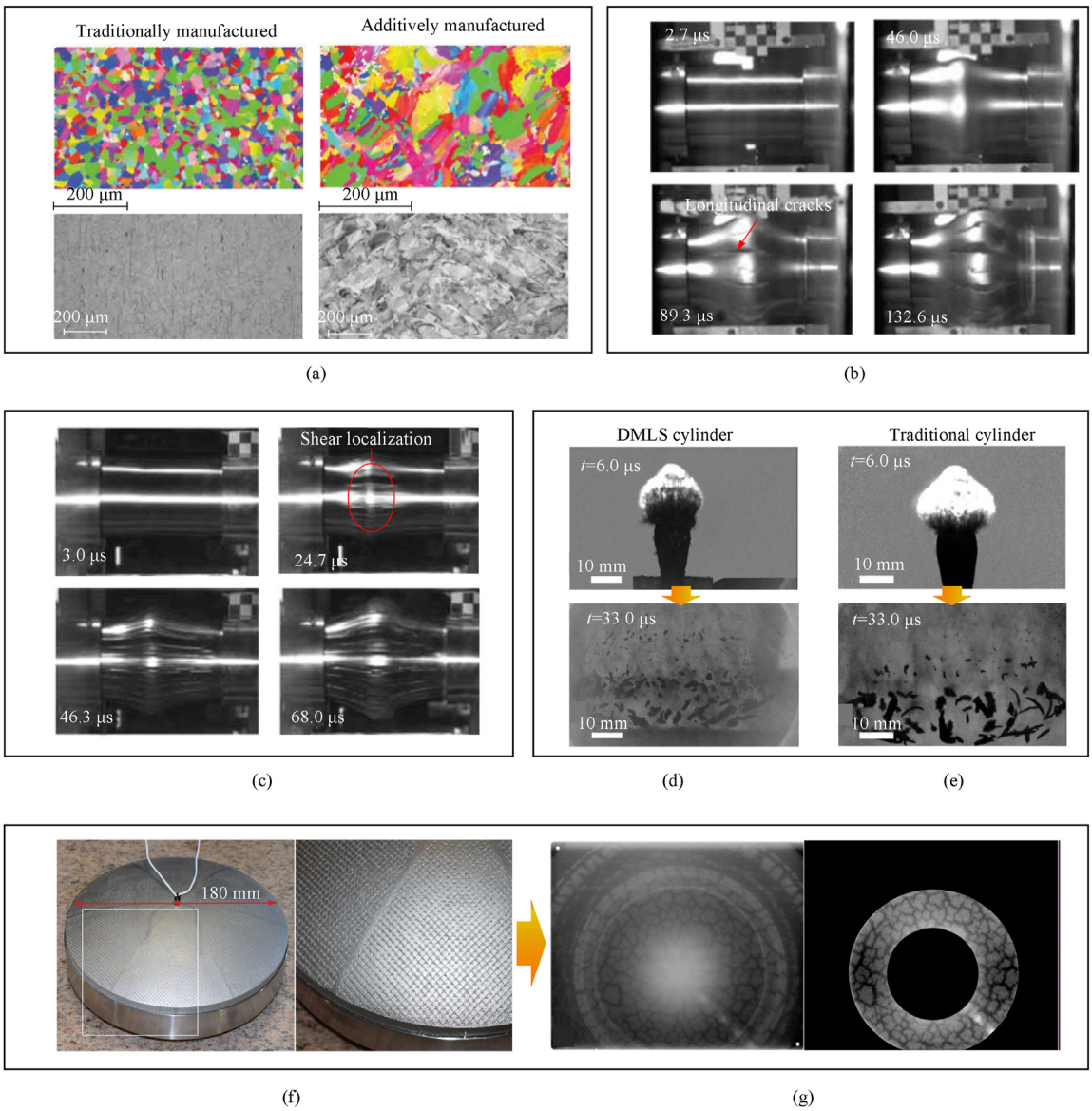

Fig. 5. (a) EBSD (top) results give the grain size and optical microscopies (bottom) show the molten pools and annealing twins. Adapted from Ref. [46]; (b) The expansion process of an SLM cylinder without defects. The longitudinal cracks are visible in the third image. Adapted from Ref. [46]; (c) The expansion and failure process of an SLM cylinder which included defects seeded during the building process. Shear localization can be seen as striations along the cylinder's length. Adapted from Ref. [46]; (d) Comparison of DMLS steel cylinder detonation events. Adapted from Ref. [47]; (e) Comparison of DMLS steel cylinder detonation events. Adapted from Ref. [47]; (f) Photographs of the AM SS316L spherical shell. Adapted from Ref. [48]; (g) Dynamic experimental radiograph acquired 60.12 μs after detonation and the radiograph highlighted region of interest. Adapted from Ref. [48].

fragmentation warhead. The fan-shaped convex structure was redesigned by combining two lattice structures of BCC-lattice and gyroid-lattice, as shown in Fig. 6(b). New structures satisfy mass symmetry and can be printed by EOS290 and IBM printers. It is feasible to manufacture the controlled warhead with excellent fragment dispersion angle and fragmentation effect by the AM technology.

3.1.3. *Preformed fragments*

Preformed fragments can have almost 100% control over the mass, shape, and size of the fragments, which is the most commonly used form of fragmentation warhead due to minimal fragmentation [56]. Xue et al. [9,57] studied the mechanical properties and ballistic performance of SLM SS316L. The average static yield strength and average tensile strength of longitudinally printed SLM SS316L were 19.8% and 28.5% lower than traditional cold-rolled SS, respectively. The cold-rolled SS also has higher dynamic compressive strength (see Fig. 7). The ballistic performance of SLM cylindrical fragments is about 8.8% lower than that of traditional fragments [9], while the ballistic performance of SLM spherical fragments is about 2.5% higher than that of traditional cold-rolled fragments [57]. Lewis et al. [58] studied the mechanical properties of AM aluminum reactive materials by using BJ technology, verifying the feasibility of AM aluminum reactive materials as warhead fragments. BJ technology is a process of selectively adding a liquid binder to a powder material to make it deposit, and more introductions can be seen in Ref. [59]. The pure aluminum samples with a certain strength and a porosity of up to 47%, the samples with Al/Si composition, and the pure aluminum samples with the addition of wax and polyurea were printed in the ExOne M-Lab printer, as shown in Fig. 8. The addition of silicon greatly reduced the melting point of the powder, which improved the strength and

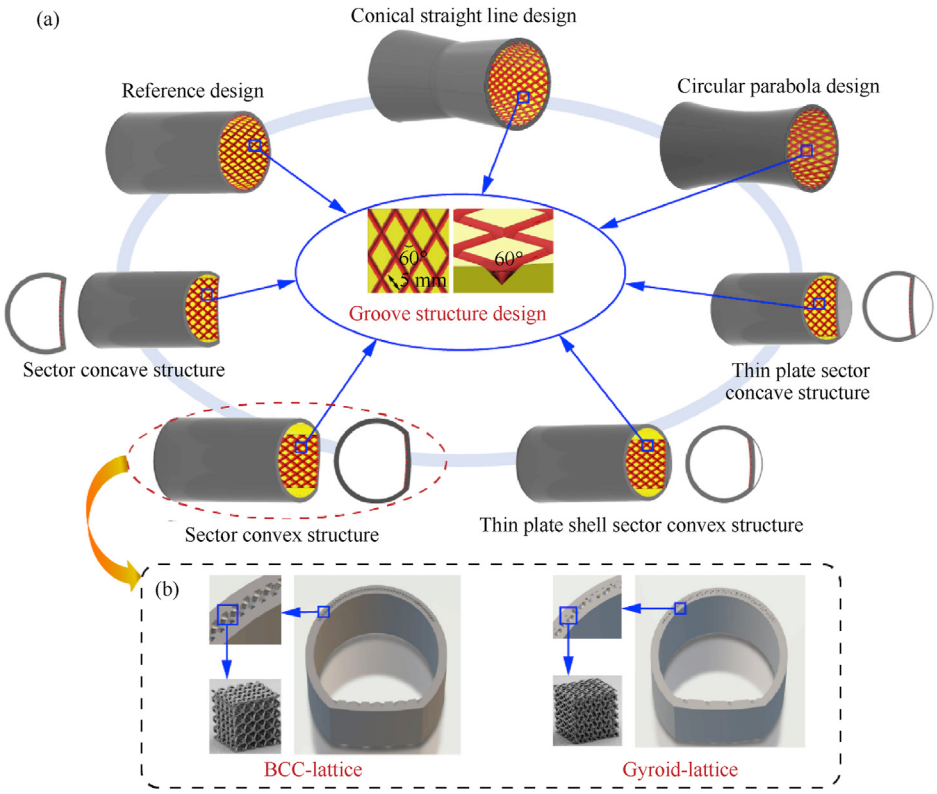

Fig. 6. (a) Seven controlled warhead shell concepts; (b) Two types of sector convex structures with two types of lattices satisfying the mass symmetry of warhead shells. Adapted from Ref. [55].

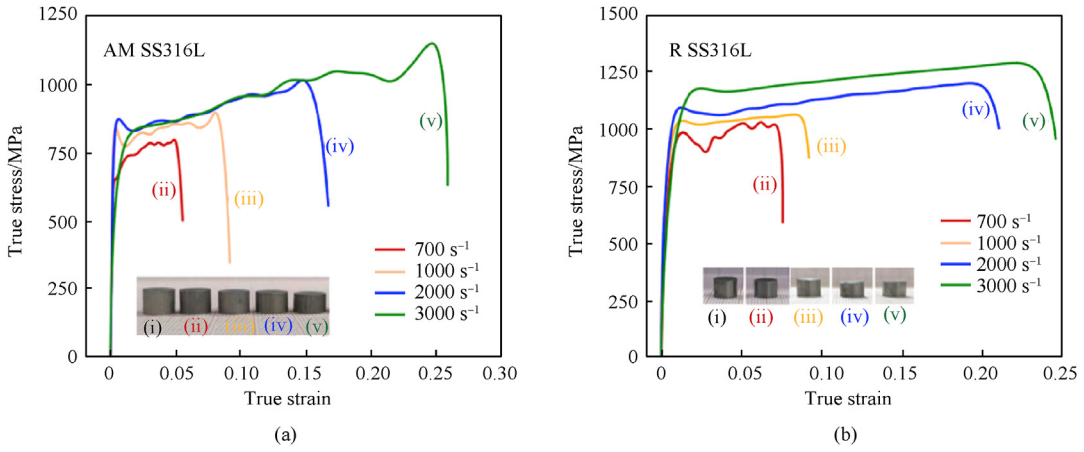

Fig. 7. The dynamic compression properties of (a) AM SS316L and (b) CR SS316L materials. Adapted from Ref. [9].

density of the samples. The pure aluminum samples with the addition of wax and polyurea exhibited good robustness under dynamic loading, despite having lower strength compared to pure metal reactive materials.

3.2. Shaped charge warhead

The liner is the damaged element of the shaped charge warhead, which is usually made of red copper, bronze alloy, high-density tantalum-tungsten alloy, and depleted uranium alloy. The manufacturing process of the traditional liner includes mechanical cutting, casting, electrochemical, powder metallurgy, hot forming, and cold working. In the actual processing process, due to the deviation in the size of liners and the structural asymmetry caused by the assembly, it is easy to weaken its energy concentration. AM technology makes it possible to design and manufacture high-precision and high-energy liners. Many studies on the application of AM in shaped charge liners have emerged, which mainly involve different materials (SS, CuSn10, etc.) and structures (solid, hollow, honeycomb, etc.). The penetration depth of the AM liners is significantly improved compared with the traditional liners. As we all know, the mechanical properties (density, strength, ductility, etc.) of the liner materials determine its penetration performance to a certain extent. However, existing research has not conducted

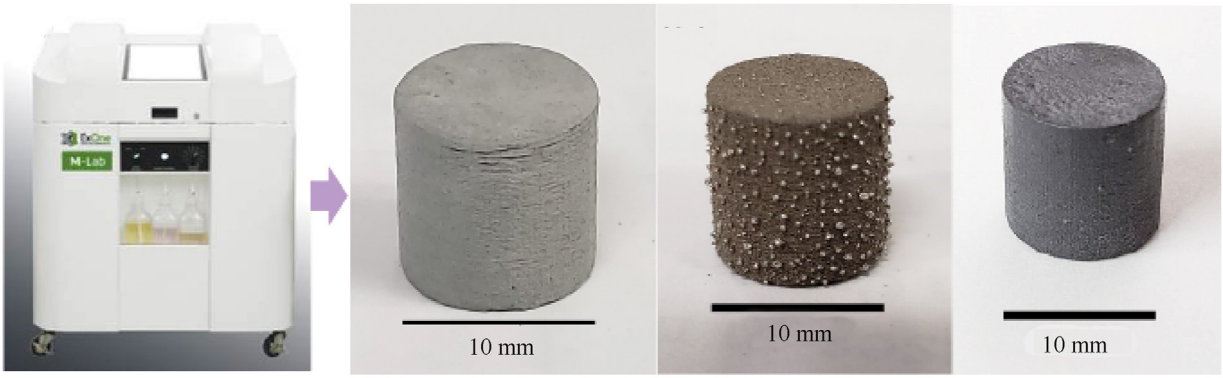

Fig. 8. (a) ExOne M-Lab 3D Printer; (b) Printed pure aluminum cylinder specimen; (c) Printed cylinder specimen with Al–Sn composition sintered at 580 °C for 2 h; (d) Printed pure aluminum specimen with the addition of wax and polyurea composition.
Adapted with permission. Copyright 2018, Naval Postgraduate School publishing [58].

detailed studies on the mechanical properties of AM liner materials. Thus the development of new AM liner materials is a direction in the future. In addition, the explosion-driven stability of the complex-structured liners is a key issue that should be paid attention to in the early stage of structural design to prevent the molding difficulty of the liners due to structural asymmetry. The relevant research on AM liners is listed in Table 3.

Mulligan et al. [60] studied the penetration performance of the conical-shaped liner printed by the SLM technology. Compared with traditional machined liners, the average penetration depth of the SLM liners was about 0.27 cm smaller than that of the machined liners. The penetration hole diameter of SLM liners for the multi-layer plates was larger than that of machined liners, as shown in Fig. 9(a). Agu et al. [61] studied the jet formation and elongation mechanism of SLS liners under a high strain rate. In contrast with the machined liner, unique precipitates were observed in the microstructure of the ending (slug) of the SLS liner, as shown in Fig. 9(b). The precipitates are likely compounds of Cr and Zr compounds, which indicates that extremely high strain deformation occurred during the formation process of the slug.

Ho et al. [62] studied the penetration ability of different structural liners printed by the SLM technology. The design and manufacturing process of liners is shown in Fig. 10(a). The stiffness and mass of the honeycomb liner can be changed by changing the wall spacing (d_1) and cell spacing (d_0) of the honeycomb structure, which is demonstrated in Fig. 10(b). In the penetration test, the hollow liner produced a maximum jet velocity of 4.2 km/s and completely penetrated the 4-layer 6.35 mm thick plates, while solid and honeycomb liners had poor penetration performance due to the higher mass and stiffness anisotropy, respectively.

Liu et al. [63] prepared SS316L liners with SLM technology in both vertical and lateral growth directions. The basic properties of vertical and lateral-grown SS316L samples are shown in Table 4. It can be concluded that the tensile strength of vertical SS316L is lower than that of lateral SS316L, but the elongation of vertical SS316L is higher. The forming condition of the vertically grown liner was better than that of the horizontally grown liner under the detonation pressure, as illustrated in Figs. 11(a) and 11(b). The penetration depth of the vertically grown liner was 21.1% higher than that of the horizontal growth at 25 times the detonation height due to the anisotropy of the AM parts. In addition, the SLM liner at 200 times the detonation height could achieve stable flight. Based on this, Song et al. [64] studied the EFP damage element forming and lethality characteristics of the 316L SS shell-cover integrated circumferential MEFP warheads manufactured by SLM technology. The overall dimensions of the MEFP warhead are Φ116 mm × 172 mm, as shown in Fig. 11(c). After the static explosion test, the AM 316L SS shell can form independent MEFP damage elements with a velocity of 1848–2112 m/s, which can penetrate a 10 mm thick A3 steel plate with a perforation diameter of 25–30 mm. Fig. 11(d) compares the flight attitude of AM 316L SS and copper material EFPs 50 μs after detonation. It can be observed that the EFP length of the former is significantly smaller than that of the latter at the same time and the head of the 316L SS EFP shows a breakage phenomenon, which is caused by the poor dynamic plasticity of the AM 316L SS materials. Guo et al. [65] studied the penetration performance of AM liners. The ballistic test results showed that the AM CuSn10 bronze liner can be used under high stress and strain conditions, and its penetration depth was 18.9% larger than that of the traditional copper liners. Sun et al. [66] also studied the microstructure and penetration performance of the CuSn10 liners made by SLM technology. The grain size of the SLM liner was observed to be smaller (around 15–50 μm) than the machined liner (200–600 μm) due to the rapid heating and cooling rate during the SLM process, as shown in Fig. 12, which contributed to improved jet performance. The penetration depth of the SLM liners was around

Table 3
Research on the application of AM technology in shaped charge warheads.

Number	Year (Country)	Technology	Liner material	Liner structure	Ref.
1	2019 (USA)	SLM	304L SS	Conical-shaped	[60]
2	2019 (UK)	SLS	CuCrZr	Conical-shaped	[61]
3	2020 (USA)	SLM	304L SS	Solid, hollow, and internal honeycomb structures	[62]
4	2020 (China)	SLM	316L SS	Vertical and lateral printed conical-shaped	[63]
5	2021 (China)	SLM	316L SS	Circumferential EFP	[64]
6	2020 (China)	SLM	CuSn10	Conical-shaped	[65]
7	2021 (China)	SLM	CuSn10	Conical-shaped	[66]

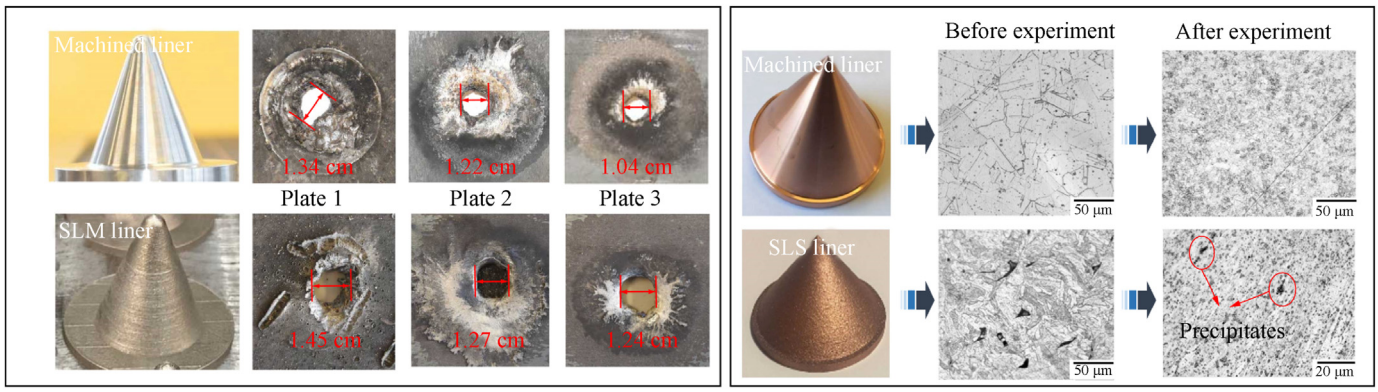

Fig. 9. (a) Comparison of average penetration hole diameters for machined and SLM liners. Adapted with permission. Copyright 2019, Proceedings of the 2019 Hypervelocity Impact Symposium publishing [60]; (b) Comparison of the microstructure of machined and SLS liner by explosive detonation. Adapted with permission. Copyright 2019, Springer Publishing [61].

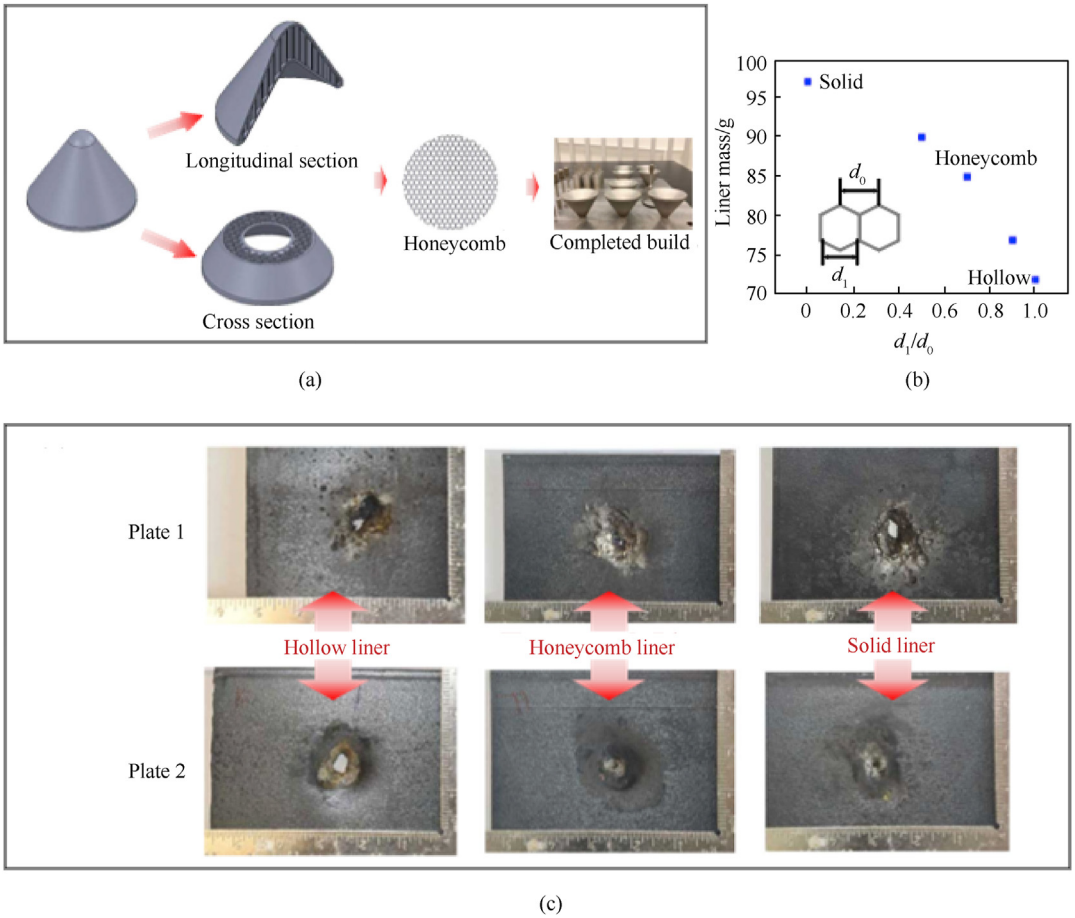

Fig. 10. (a) Design route of SLM liner; (b) Dependence of the conical liner mass on honeycomb parameters; (c) Images of impact craters from the first two layers using hollow, honeycomb, and solid liners.
Adapted from Ref. [62].

Table 4
The basic properties of vertical and lateral grown SS316L samples [63].

Printing direction	Density/(g·cm^{-3})	Tensile strength/MPa	Elongation/%
Vertical printing	7.93	660	38
Lateral printing	7.92	734	29

27% larger than that formed by the traditional cast CuSn10 liners in the penetration test.

3.3. Penetrating warhead

Penetrating warhead design has to deal with two contradictory

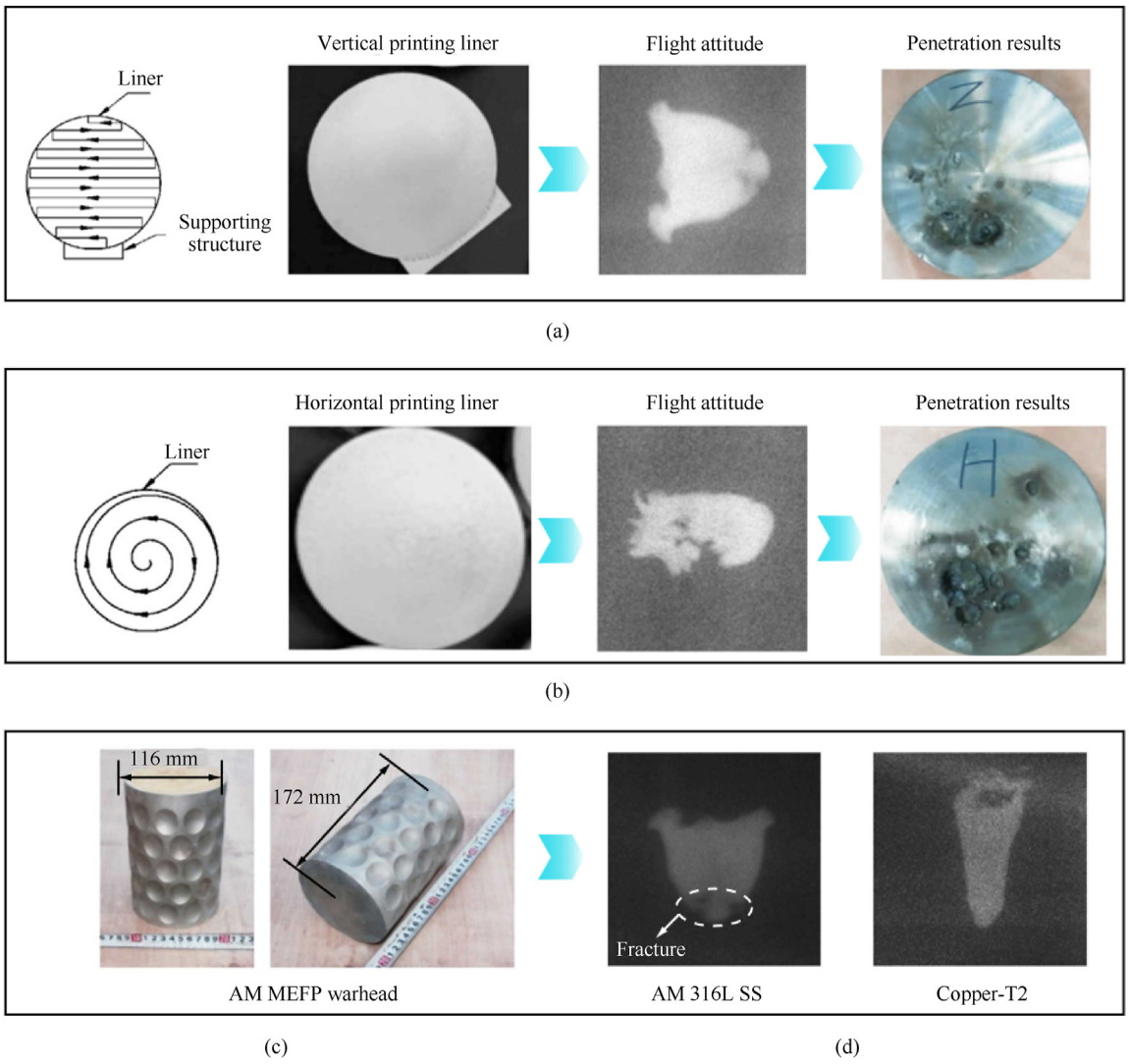

Fig. 11. Flight attitude and penetration results of vertically printed (a) and horizontally printed (b) liners. Adapted from Ref. [63]; (c) Structure of AM MEFP warhead; (d) Comparison of the flight attitude of 316L SS and copper EFP after 50 μs detonation.

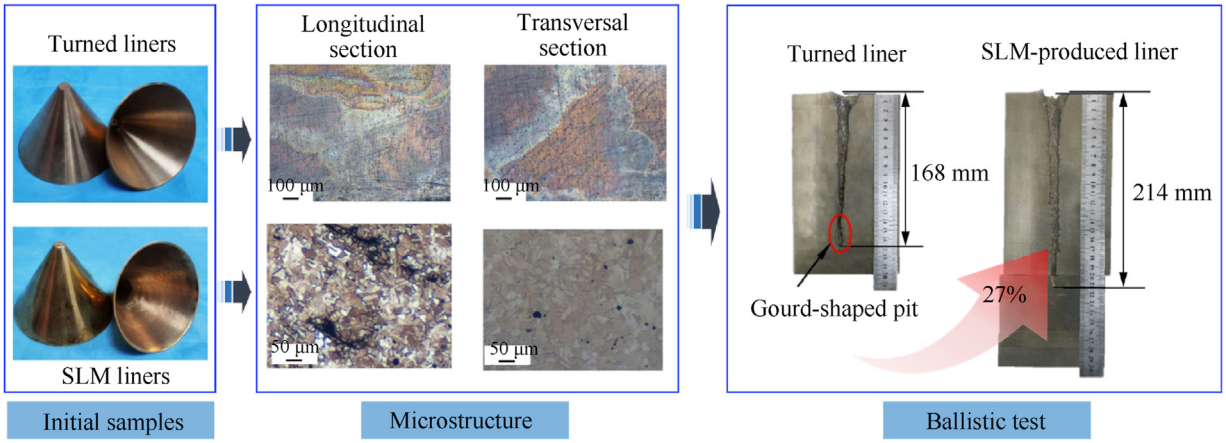

Fig. 12. Microstructure and penetration capability of turned liner and SLM liner by Sun et al. Adapted from Ref. [66].

goals: high penetration ability and high blast effect. On the one hand, high penetration capabilities often require the use of shells

Table 5
Typical research on laser AM WHAs.

Composition	Method	Density/(g·cm^{-3})	Mechanical properties	Existing problems	Ref.
90W–7Ni–3Fe	DED	–	650 MPa (0.2 YS); 5.2% (elongation)	Poor plasticity and high porosity	[68]
50W–Ni–Fe	LMD	12.8	737 MPa (0.2 YS)	–	[69]
75W–Ni–Fe	LMD	15.9	956 MPa (0.2 YS)	–	[69]
90W–7Ni–3Fe	LMD	> 17.0	–	–	[70]
90W–7Ni–3Fe	LMD	17.0 ± 0.24	822 ± 30 MPa (0.2 YS)	–	[71]
90W–7Ni–3Fe	SLM	Full densification	1121 MPa (0.2 YS); < 1% (elongation)	Poor elongation	[72]
70W–18Ni–6Fe–6Co	SLM	16.3	7%–9.5% (elongation)	–	[73]

*Note: The "0.2 YS" means the "0.2% yield strength", and "-" indicates that the study does not give corresponding information.

with high density, high strength, and a certain degree of plasticity. On the other hand, high explosive effects require the filling of more explosives while ensuring penetration capabilities. We roughly summarize the new penetration materials manufactured by AM technology, which can be used in penetrating warhead shells. For the latter, related research on lattice penetrators based on AM technology and TO methods has been also widely reported.

3.3.1. New penetrating materials

The WHAs are considered ideal materials for penetrating warhead shells and are the most commonly used materials. Since tungsten itself has a high ductile-to-brittle transition temperature (DBTT) (−200–400 °C), microcracks and brittleness have always been problems that prevent successful printing of WHAs. Research on using laser AM technology to print WHAs with W–Ni–Fe composition is summarized in Table 5. It can be seen that the low plasticity is the main problem. Although many methods such as alloying, scanning strategy adjustment, remelting, and substrate heating have been used to mitigate cracks [67], this is still difficult at present. Therefore, most studies still focus on the static mechanical properties of AM WHAs. There is no doubt that AM WHAs that can be applied to penetrating warheads still face great challenges.

Amorphous alloys, also known as metallic glass, are liquid superheated melts formed in the process of rapid cooling. Their liquid structural characteristics are retained and have many characteristics of metals and glasses simultaneously. Adiabatic shear self-sharpening of bulk metallic glasses (BMGs) was first found in zirconium alloys with a density of about 6.7 g/cm^3 [74,75], yet it was ineffective for penetrating materials due to the lower density. Therefore, the combination of BMGs with high-density metals, such as tungsten fiber and carbon steel fiber, could achieve ideal density and deformation effects. It has been reported that the density of tungsten zirconium-based bulk metallic glass could reach 17.1 g/cm^3 [76], exhibiting obvious self-sharpening behavior during the penetration process. Various methods such as PBF [77,78] and DED have been used to manufacture AM metallic glasses.

The multi-principal HEAs proposed by Yeh [79] broke through the traditional alloy design concept. The HEA is a kind of alloy with high mixing entropy formed by alloying more than five elements

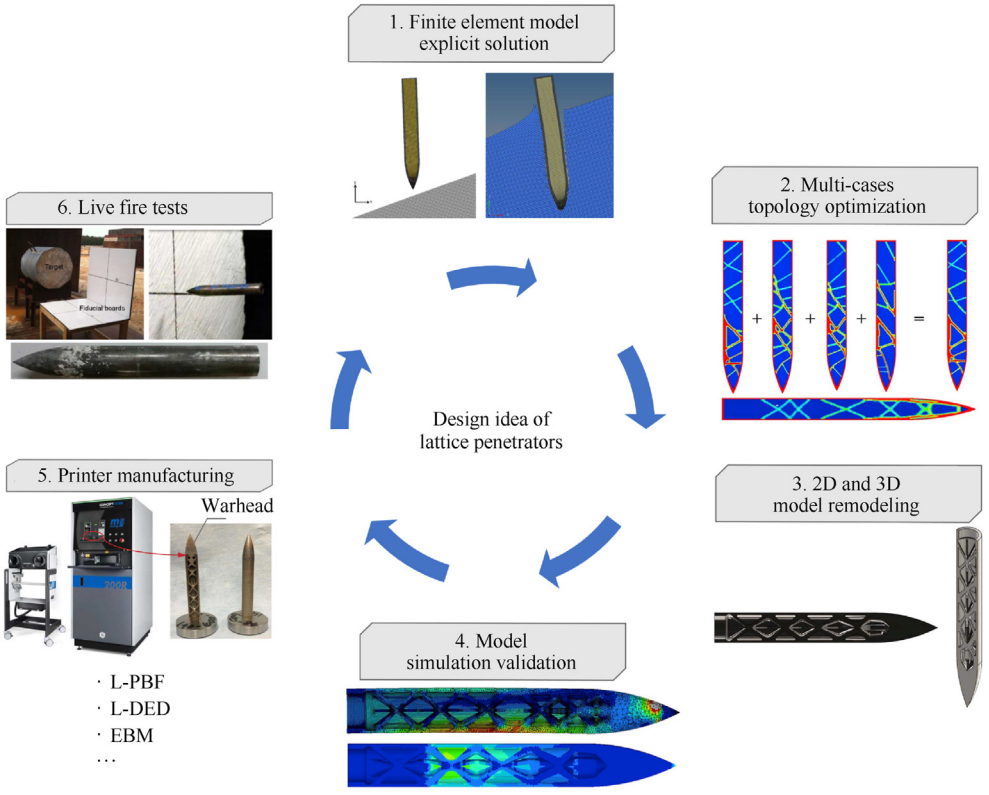

Fig. 13. The idea of AM combined with the TO method to manufacture lattice penetrator. Adapted from Ref. [88].

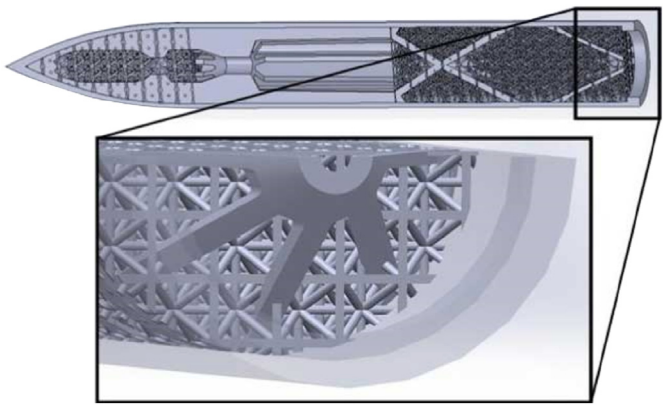

Fig. 14. Lattice penetrator as conceived by Richards. Adapted from Ref. [87].

according to the equiatomic ratio or near equiatomic ratio. HEAs have excellent properties such as high strength, high hardness, high wear resistance, high oxidation resistance, and high corrosion resistance. It has been found that HEAs, such as the HfNbZrTi and WFeNiMo, have unique advantages in the ballistic application [76,80–82] due to the severely local adiabatic deformation ability and high shear sensitivity. The LMD and SLM technologies are mainly adopted to manufacture HEAs [83]. Zhang et al. [84] published the first research on AM CoCrCuFeNi HEAs in 2011. Since 2018, a large number of studies on HEAs manufactured by SLM technology have appeared. Brif et al. [85] studied the manufacturing process of HEAs by SLM technology using gas-atomized pre-alloyed powders. An equiatomic CoCrFeNi HEA with a strength of 745 MPa and a ductility of 32% was fabricated. The SLM CoCrFeNi HEA reported by Kuzminova et al. [86] had twice the yield strength of conventional hot-rolled samples in the range of 150 °C–300 °C.

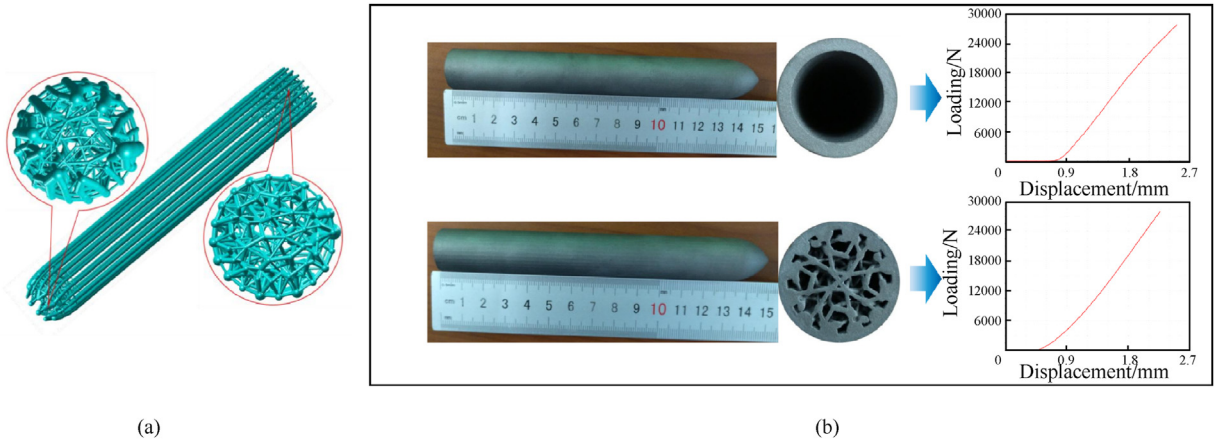

Fig. 15. (a) The TO result of the scaled model of GBU-28; (b) Physical pictures of unoptimized and optimized warheads and their compression loading-displacement curves. Adapted from Ref. [89].

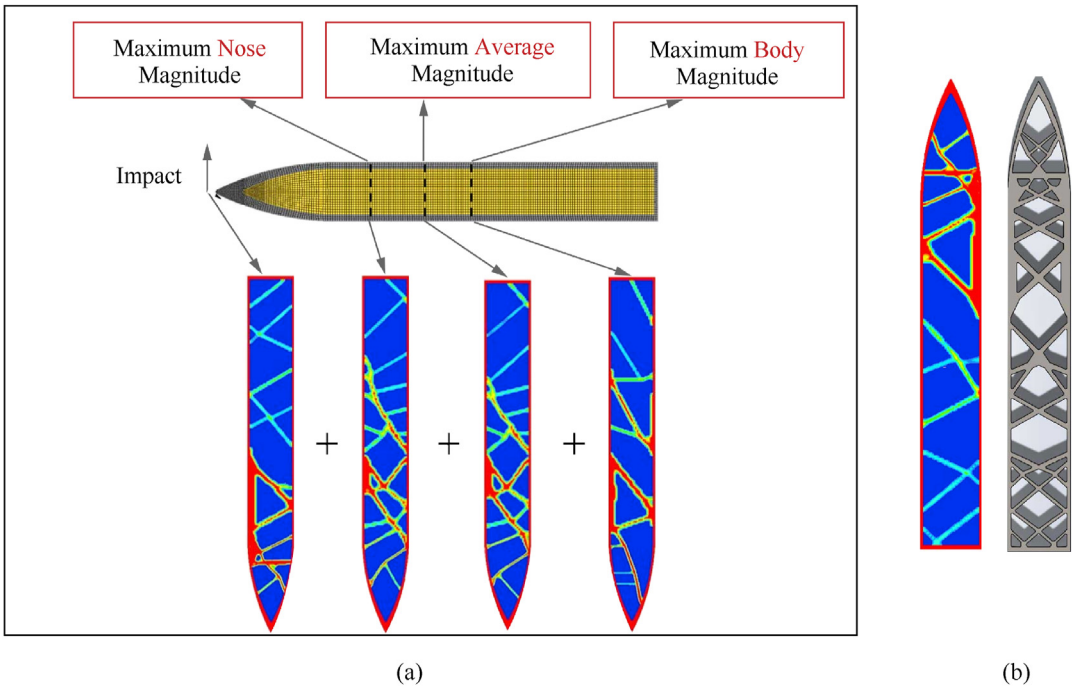

Fig. 16. (a) Location determination of the four load steps applied to the penetrator during multi-case TO simulation; (b) Simulation results of multi-case TO and the structure after 2D model reshaping.
Adapted from Ref. [90].

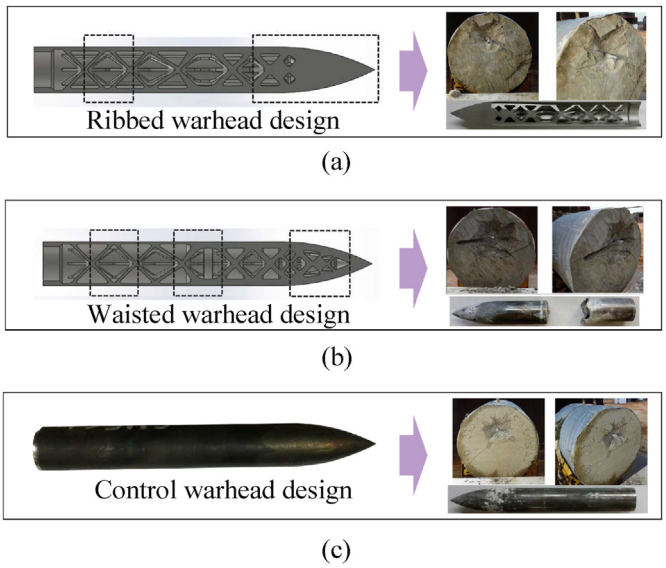

Fig. 17. (a) The impact test results of the ribbed design warhead; (b) The impact test results of the waisted design warhead; (c) The impact test results of the control design warhead.
Adapted from Ref. [91].

3.3.2. Lattice penetrator

3.3.2.1. Concepts and ideas. The traditional penetrating warhead often has a thick shell to ensure enough strength. Through the projectile structure optimization, the thick shell can be thinned and the shell strength can be improved. The thin shell can increase the amount of explosives when the volume of the warhead is constant, which can achieve a better fragmentation effect. Since structurally optimized projectiles usually have a lattice structure, they are called lattice penetrators. The research ideas of the lattice penetrator are shown in Fig. 13. It is divided into six steps, in which the TO method plays an important role during the design process. The conceptualization of an AM lattice penetrator was first proposed by Richards et al. [87] in 2015. A lattice penetrator was designed by using the single subcase TO method and the overall strength of the penetrator was expected to be increased by filling the space inside the warhead with a lattice structure, as shown in Fig. 14.

3.3.2.2. Test verification of lattice warhead. Different types of lattice warheads have been designed based on the TO method. Jing et al. [89] proposed a lattice structure TO method using the diameter of the rod unit in the lattice structure as the design variable. Taking the scaled model of GBU-28 as an example, the TO result was obtained in Fig. 15(a). The optimized warhead has a thinner shell, which can make the warhead produce smaller fragments after penetrating the target. The unoptimized and optimized warheads (made of Ti–6Al–4V material) were printed by SLM technology. The masses of the two are 80.9 g and 81.7 g respectively, with a difference of only 0.98%, but the optimized warhead wall thickness is reduced by 37.5%. The compression test results also showed that the stiffness of the optimized warhead increased by 5.3%, as shown in Fig. 15(b). Although a direct ballistic impact test has not yet been carried out, existing research has shown the potential of optimized warheads in a penetration event.

Researchers from the U.S. Air Force Institute of Technology have conducted numerous works by combining the TO method and AM technology. They adopted 15-5 PH SS for preliminary experimental verification due to the maturity of AM technology in manufacturing steel materials. Graves et al. [90] conducted the multi-case TO simulation. The acceleration changes of the warhead nodes at different times were determined through the explicit dynamics simulation of the warhead penetrating the concrete target and four load steps were also determined after obtaining four positions on the warhead with large force change. The final warhead structure was obtained in Fig. 16(b). Graves et al. [91] reshaped this structure by symmetrical rotation operation and obtained two types of 3D warhead models. One was the "waisted" design, which adopted a thickened wall design at the contact between the thin wall and the internal lattice, contributing to resisting the bending loads in the penetration process. However, there may be a stress concentration phenomenon in the transition zone between the thick wall and the thin wall. The other was a "ribbed" design that eliminated the thick-walled area at the contact and replaced the warhead area with a solid. Two types of lattice penetrators were manufactured by using DMLS technology. The penetrating warhead without the lattice structure inside the shell was printed as a control group. Three structural penetrators penetrated the concrete target with the same initial velocity. The results showed that the penetrators of the control design and the "ribbed" design survived in both vertical penetration and oblique penetration (20° inclination) conditions. Although the penetration depth of the "ribbed" design was about 10% lower than that of the control warhead, two types of penetrators remained intact. The "waisted" design warhead broke

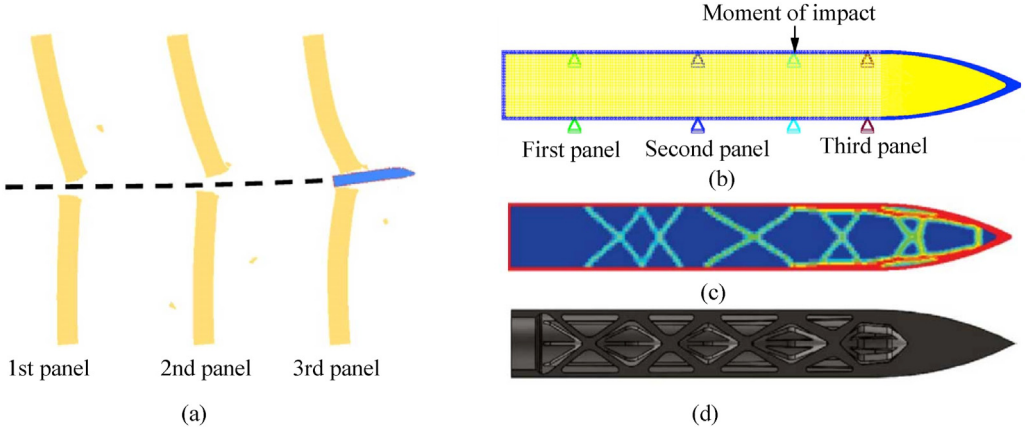

Fig. 18. (a) Visualization of four critical time conditions in the simulation; (b) The boundary conditions for the four different critical time steps; (c) The TO density plot result. The red represents fully dense elements and the blue represents void space; (d) Final optimized structure after the model remodeling.
Adapted from Ref. [88].

somewhere in the middle due to the sharp change of stiffness in the transition zone between thick and thin walls, as illustrated in Fig. 17. Graves's research results showed that the penetrating warhead structure can be designed to meet the printing requirements by the TO method combined with the corresponding engineering conditions.

Moreover, whether AM lattice penetrators with a thinner shell could survive an impact that contained multiple targets became a research interest of the US Air Force. Provchy et al. [88,92] developed a method of designing an optimized system that is capable of interacting with a multi-layered target. The coordinated acceleration response of the nose and tail of the penetrators allows critical time steps to be chosen based on the maximum average acceleration of the penetrators as a whole. Four critical time steps with the corresponding forces and boundary conditions were identified and used to imply a multi-case TO, as shown in Figs. 18(a) and 18(b). The optimization contour and model reshaping results were obtained, as shown in Figs. 18(c) and 18(d). Based on the work of Provchy et al., Patel et al. [93] studied the impact of hybrid material penetrators on multi-layer concrete targets. By improving the weighted compliance method in TO simulation [94], the method for developing AM lattice penetrators for specific target sets was extended, and the lethality of the hybrid penetrators was also improved while maintaining the stiffness of the penetrator during the perforation process. A hybrid material penetrator was obtained, including a thin steel shell and a topologically optimized aluminum internal structure, as shown in Fig. 19(a). It is worth mentioning that the material inside and outside the warhead can be customized for different targets. Finally, the live fire testing for the hybrid material penetrators was performed. It was ultimately found that the nose of the penetrator fails catastrophically as in Fig. 19(b), while the insert can be seen surviving at the midpoint of the penetrator.

For the composite penetrators in Fig. 19(a), Beard et al. [95] studied the influence of alternative materials for the composite penetrator casings on penetration capabilities in 2020. Steel, tungsten, and silicon-carbide-reinforced aluminum were used as the outer and inner shell materials of the sandwich construction. The core material was created using AM of Inconel 718 with a three-period minimum surface (TPMS) [96] to provide the penetrator shell with high stiffness and strength while reducing the materials. Hereafter, the penetration performance of composite penetrators for different types of target plates (steel, aluminum, and concrete) was numerically investigated. This study explored whether a completely new penetrator configuration could match or exceed the performance of an SS penetrator with a similar size and shape. Limido et al. [97] also studied the potential of penetrators with lattice structures to penetrate concrete targets. Their purpose was to design penetrators with lattice structures and to ensure good mechanical strength (survivability) and penetration performance while reducing the weight of the warhead. By conducting compression tests on the 'diamond' and 'octet' truss structures, the 'octet' structure with greater yield strength was selected to be inserted into the warhead. The reference and lattice structure warheads were manufactured and shown in Fig. 20, which were made of 17-4 PH SS materials. The weight of the warhead with a lattice structure was about 15% lighter than that of the reference

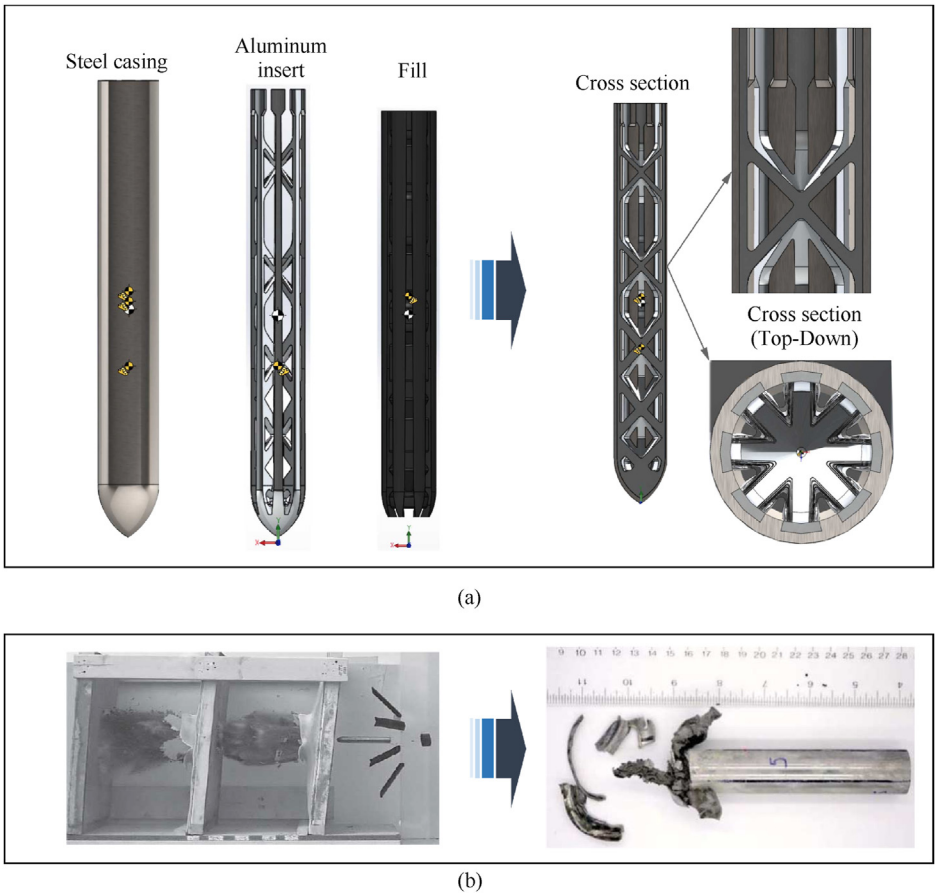

Fig. 19. (a) The final optimized design; (b) A snapshot of the penetrator penetrating the target and the recovered penetrator after the live fire testing. Adapted from Refs. [93,94].

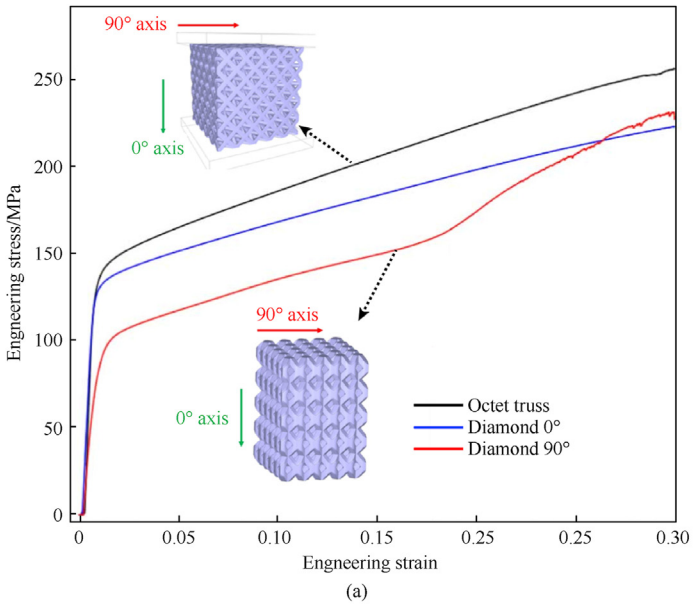

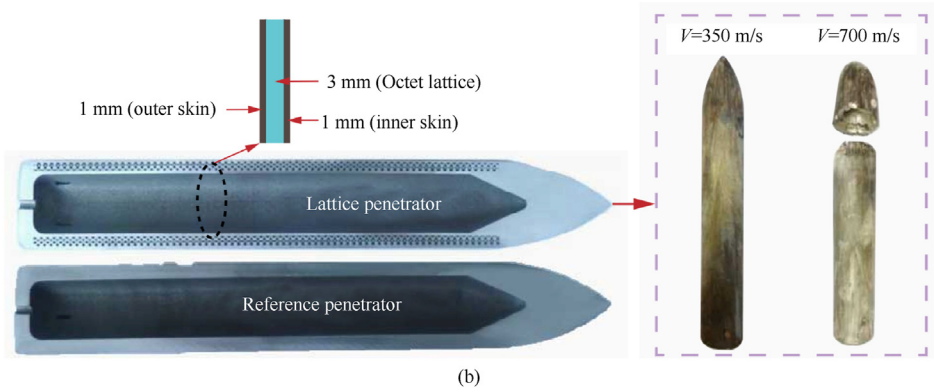

Fig. 20. (a) Two lattice structures and their compression stress-strain curves; (b) Two structural penetrators (lattice and reference penetrator) by Limido et al. and the recovered penetrators at 350 m/s and 700 m/s velocities.
Adapted from Ref. [97].

solid warhead. When penetrating the concrete target at 350 m/s, the complete warhead was recovered. The warhead after penetrating the target plate failed until the increasing velocity reached 700 m/s.

3.3.2.3. Reactive material-filled lattice warhead. With the availability of manufacturable lattice penetrator structures, survivability in impact events has been confirmed by most studies. A new idea is to fill the interior of the lattice penetrator with reactive explosives

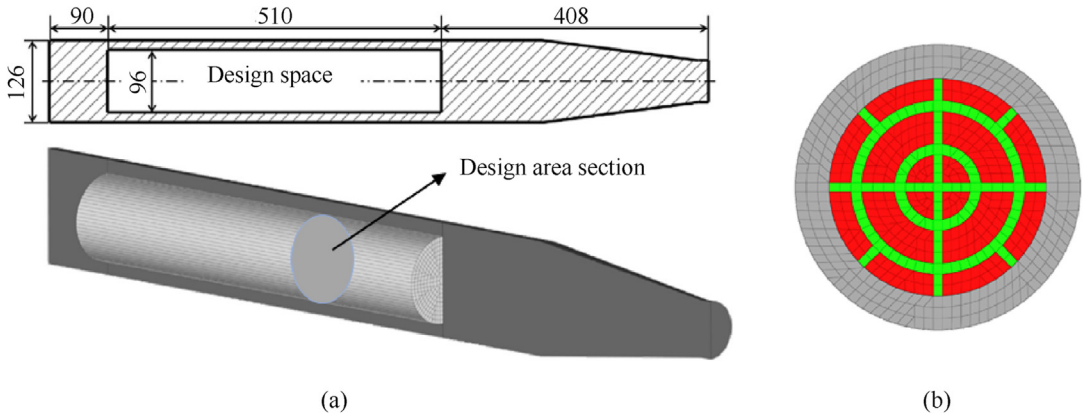

Fig. 21. (a) Design space for TO; (b) Cross-sectional structure after TO simulation, and the green part is the retained structure and the red part is the removal part.
Adapted from Ref. [98].

to further improve its impact resistance and energy capacity. Kim et al. [98] developed a design optimization method for the reactive material structure (RMS) and performed the TO of the RMS of the penetrating warhead (see Fig. 21(a)). A finite element method for penetration analysis was used to evaluate the impact resistance of the warhead structure, and the simulation results were verified by comparison with experimental results. On this basis, the TO method was introduced to determine the shape of the structure, and finally, the cross-sectional structure of the RMS was obtained, as shown in Fig. 21(b). However, the actual performances of the optimum design are not investigated through experiments in the study.

4. Application of AM in warhead charge

The traditional manufacturing methods of warhead charges include cast-cure, melt-cast, and press powders methods. All three methods have their disadvantages. The cast-cure method may cause problems such as ingredient settlement, poor bonding between the casting material and the shell, and shrinkage cracking during the manufacturing process. In addition to the problem of shrinkage and cracking, the melt-casting method may also cause irreversible volume growth of the explosive and poor accuracy. Although the press powders method does not have the above shortcomings, it is not suitable for large-size charges and ammunition molding with complex internal channels. Therefore, AM technology is expected to realize the molding and manufacturing of high-precision, large-size, and complex charges for warheads. AM technology mainly changes warhead charges in terms of materials and structures. On the one hand, AM technology can efficiently adjust the explosive formula and fundamentally achieve high energy of explosives. On the other hand, AM technology can precisely control the structure of the explosives to change the detonation effect. Therefore, energy-customized AM explosives will be a research direction with great potential and the relevant progress is introduced as follows.

4.1. New high-energy and insensitive explosives

High energy and low sensitivity are the eternal pursuit of explosives. Traditional explosives have experienced three generations of development: nitroglycerin, TNT-based, and RDX-based, and are currently developing towards the fourth-generation explosive CL-20. As the generation of explosives increases, the energy becomes higher and higher, and the cost becomes relatively higher. Researchers began to try to use AM technology to create lower-cost high-energy explosives. At present, most studies have shown that the performance of AM explosives reached or exceeded that of traditionally manufactured explosives, although no engineering application has been found yet.

Xiao et al. [99,100] prepared a TNT/nano HMX melt-cast explosive grain (φ20 mm × 20 mm) composed of 60 wt% TNT and 40 wt% superfine HMX by using an FDM 3D printer, as shown in Fig. 22. The printed grains reached 98.6% of the theoretical density, and the compressive strength and tensile strength of grains were 87.5% and 66.7% higher than the traditional cast ones, respectively. Besides, the microstructures of top and side views demonstrate the anisotropy of the printed grains. The fracture surface of printed grains was smooth and dense and the superfine HMX particles were uniformly mixed with TNT without any defects, while many holes can be observed inside the cast grains, which greatly reduces the density and mechanical properties of the grains, as shown in Figs. 22(c) and 22(d). Zong et al. [101] successfully designed and fabricated a ring-structured TNT/HMX-based explosive grain with an FDM 3D printer. The printing process and microstructures of the grain are presented in Fig. 23(a), from which a dense microstructure for the printed grain can be observed. Ruz-Nuglo et al. [102] printed different types of simulated polymer-bonded explosives,

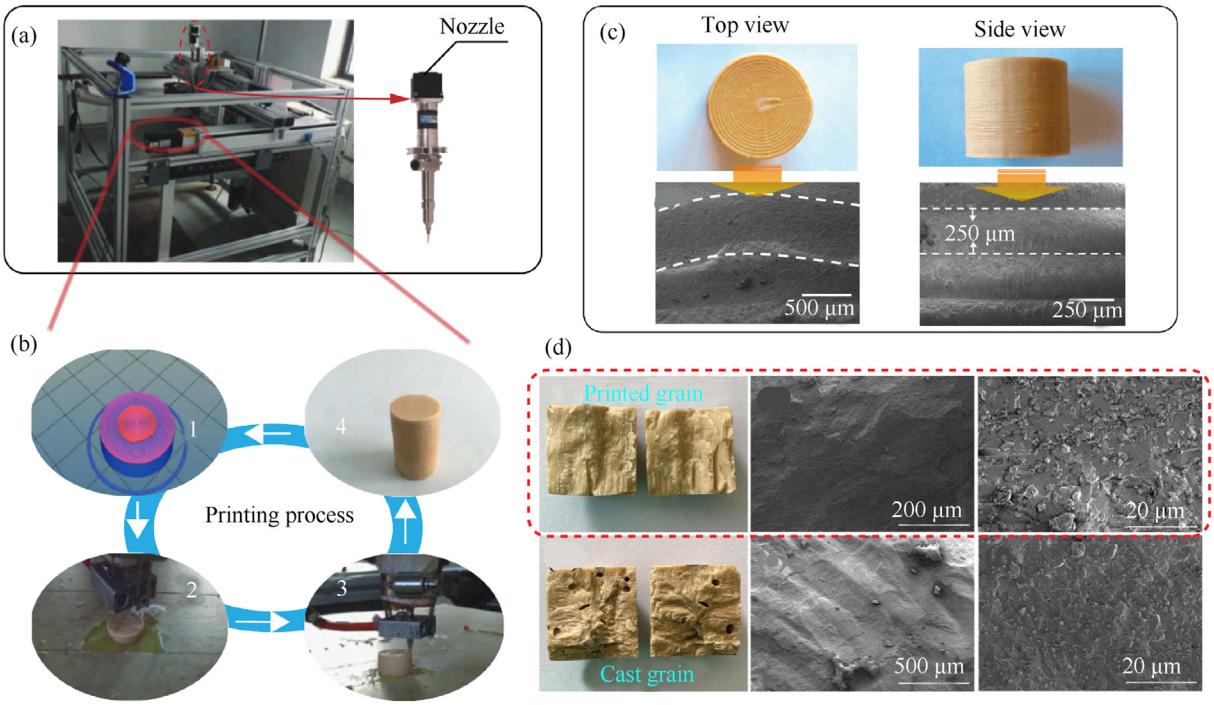

Fig. 22. (a) The FDM printer made by Xiao et al.; (b) The printing process of TNT/nano HMX melt-cast explosive grain; (c) The top and side views of printed samples; (d) Microstructure of fracture surfaces of printed and traditional explosive samples.
Adapted from Refs. [99,100].

Sylgard®, tetrafluoroethylene, hexafluoropropylene, and vinylidene fluoride (THV) polymer inks by the DIW technology. The free-standing films and structures with particle loadings up to 85 wt% could be achieved using the appropriate inks, making DIW promising for AM of polymer-bonded reactants. Zhang et al. [103] designed a CL-20-based explosive ink, and the smooth explosive film was prepared using the micro-jet DIW technology, with a critical diameter of 0.153 mm and an average detonation velocity of 8090 m/s.

An's team at the North University of China has carried out extensive work on using AM technology to fabricate high-energy explosives. An et al. [105] prepared a CL-20-based composite with a high density and low impact sensitivity by using DIW technology. Its critical detonation size was around 0.4 mm, which contributed to the detonation at the micro level to a certain degree. Hereafter, An et al. [106] obtained CL-20-based composite by using the method of preparing the emulson, combined DIW technology load explosive ink in the condition of micro size. It had fewer internal defects and reduced impact sensitivity after testing. Its critical size of detonation and the detonation velocity were around 0.17 mm and 8079 m/s, respectively. A 3,4-dinitrofurazanofuroxan (DNTF) based composite with nitrocotton (NC) and Viton as binders was prepared [107]. The composite had spheroidal particles with sizes ranging from 1 μm to 2 μm and it had a lower impact sensitivity and higher thermal stability compared with raw DNTF. Additionally, the composites also exhibited excellent detonation properties, whose critical size of the detonation was around 0.01 mm and the average detonation velocity was 8580 m/s at the charging width of 1 mm. An' team [104] designed a new type of UV-curing explosive ink formulation using unsaturated polyester as the binder, styrene as the active monomer, 2,4,6-trimethylbenzoyl-diphenylphosphine oxide as photoinitiator, CL-20 as the main explosive. The microstructure, safety performance, and explosive transfer performance of the explosive ink molded samples were tested and analyzed. The results showed that the composite materials have a fast curing molding speed. The surface of the explosive ink molded sample is smooth and flat, but some holes can be observed under higher magnification (Fig. 23(b)), which is caused by the numerous thermal radiation of the general ultraviolet light source. The CL-20 particles are uniformly distributed and are connected by a binder to form a honeycomb structure, which is conducive to the propagation of detonation waves under micro-size conditions. The characteristics drop height of the molded sample reached 39.8 cm (about 3 times higher than the raw material), indicating higher safety. The detonation velocity of the molded sample is 7129 m/s at a density of 1.612 g/cm^3, exhibiting a good detonation performance under micro-size conditions.

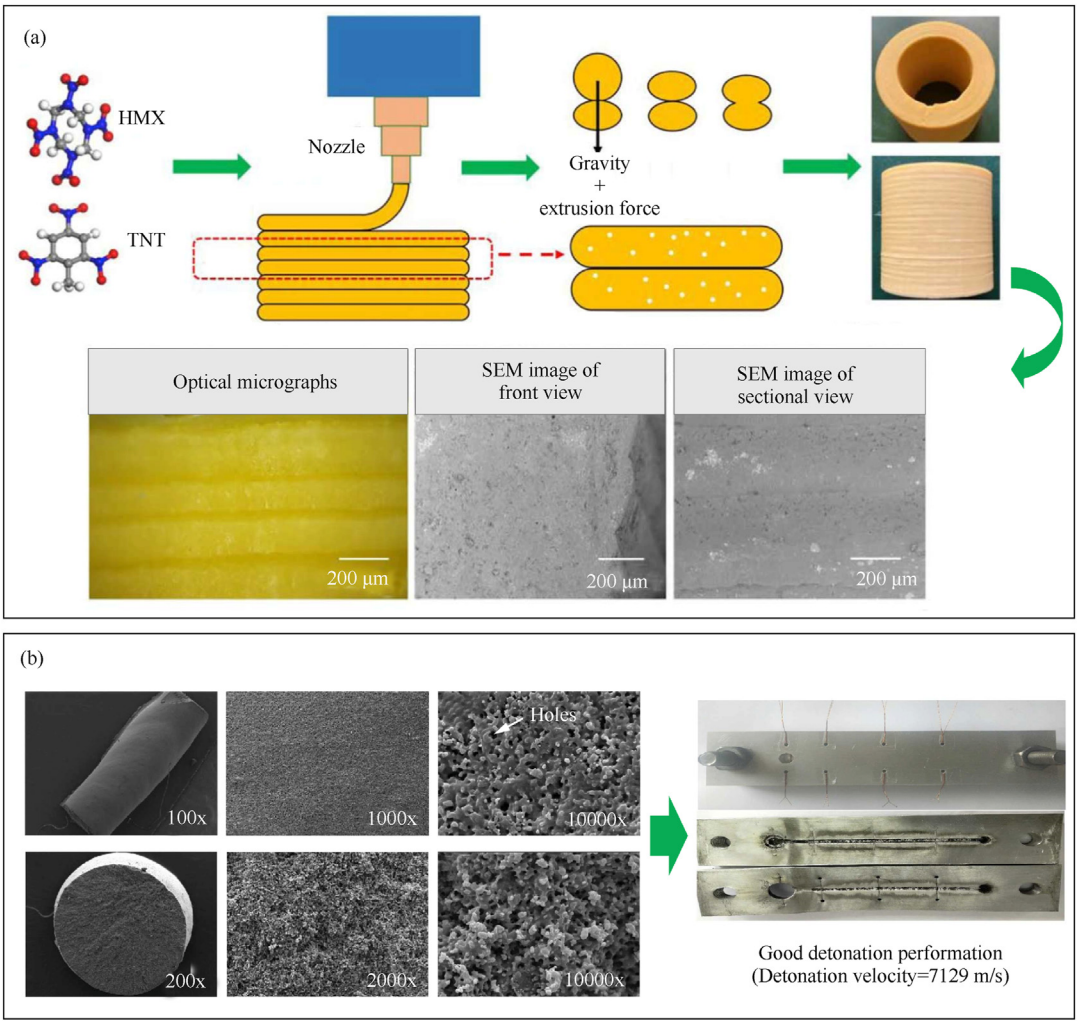

Fig. 23. (a) Flow chart of 3D printed ring-structured TNT/HMX-based explosive grain and the microstructure of samples at different positions. Adapted from Ref. [101]; (b) SEM images of the surface and cross-section of CL-20-based composite, and photographs of CL-20-based composite before and after detonation. Adapted from Ref. [104].

4.2. High-precision and energy-customized explosives

The ability to precisely change the structure of explosives is a unique advantage of AM technology, which is expected to enable the customization of explosive energy. New structures of explosives, such as internal hollow structures, gradient structures, and honeycomb structures, have been reported in numerous literatures. Existing research shows that related work is still theoretical and laboratory-level preparation.

4.2.1. Internal hollow structures

Los Alamos scientists have theoretically demonstrated how to control the behavior of explosives by manipulating their microstructure [108]. In a proof-of-concept simulation test, a cylinder composed of a high explosive (HE) material with varying radial void density was impacted. The higher the void density, the faster the shock wave propagates. Finally, their control of the detonation front showed a clear sinusoidal shape, as shown in Fig. 24(a), confirming a new level of control. AM technology can precisely control the hollow structure inside the explosive and customize the detonation effect of the explosive.

Brown et al. [109] proposed switchable HEs as a new class of energetic material. They create a HE lattice composed of the 73 wt% octahedron-1,3,5,7-tetranitro-1,3,5,7-tetrazine (HMX)-based AMX 7301 ink formulation by utilizing AM technology. The HE lattices can only be detonated after being filled with a mechanically activating fluid, otherwise, it cannot be detonated. By analyzing the detonation velocity and Gurney energy of HEs, Brown et al. evaluated the performance of fluid-filled AM HE lattices. The Gurney energy of the unfilled lattice was 98% lower than that of the equivalent water-filled lattice. Moreover, by changing the mechanical properties of the fluid, the Gurney energy and detonation velocity of the explosive can be adjusted by 8.5% and 13.4%. This study attributes the switching capabilities of HEs to critical diameter effects, as illustrated in Fig. 24(b). Fig. 24(c) shows the computer-generated model of the AM HE structure and surface

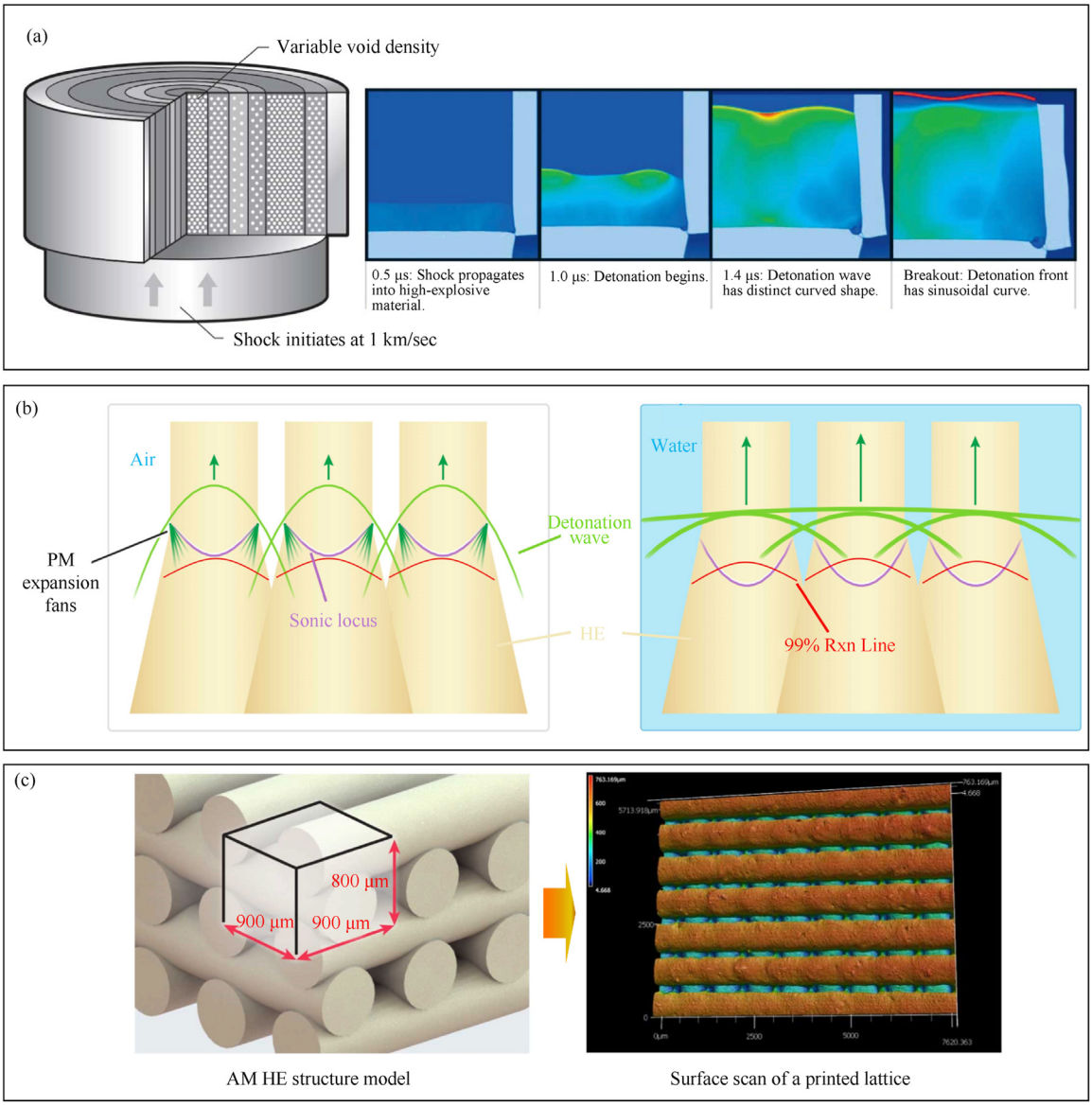

Fig. 24. (a) Los Alamos scientists' concept simulation test. Adapted from Ref. [108]; (b) Detonative switching effects in HE lattices; (c) Computer-generated model of AM HE structure and surface scan of a printed lattice. Adapted from Ref. [109].

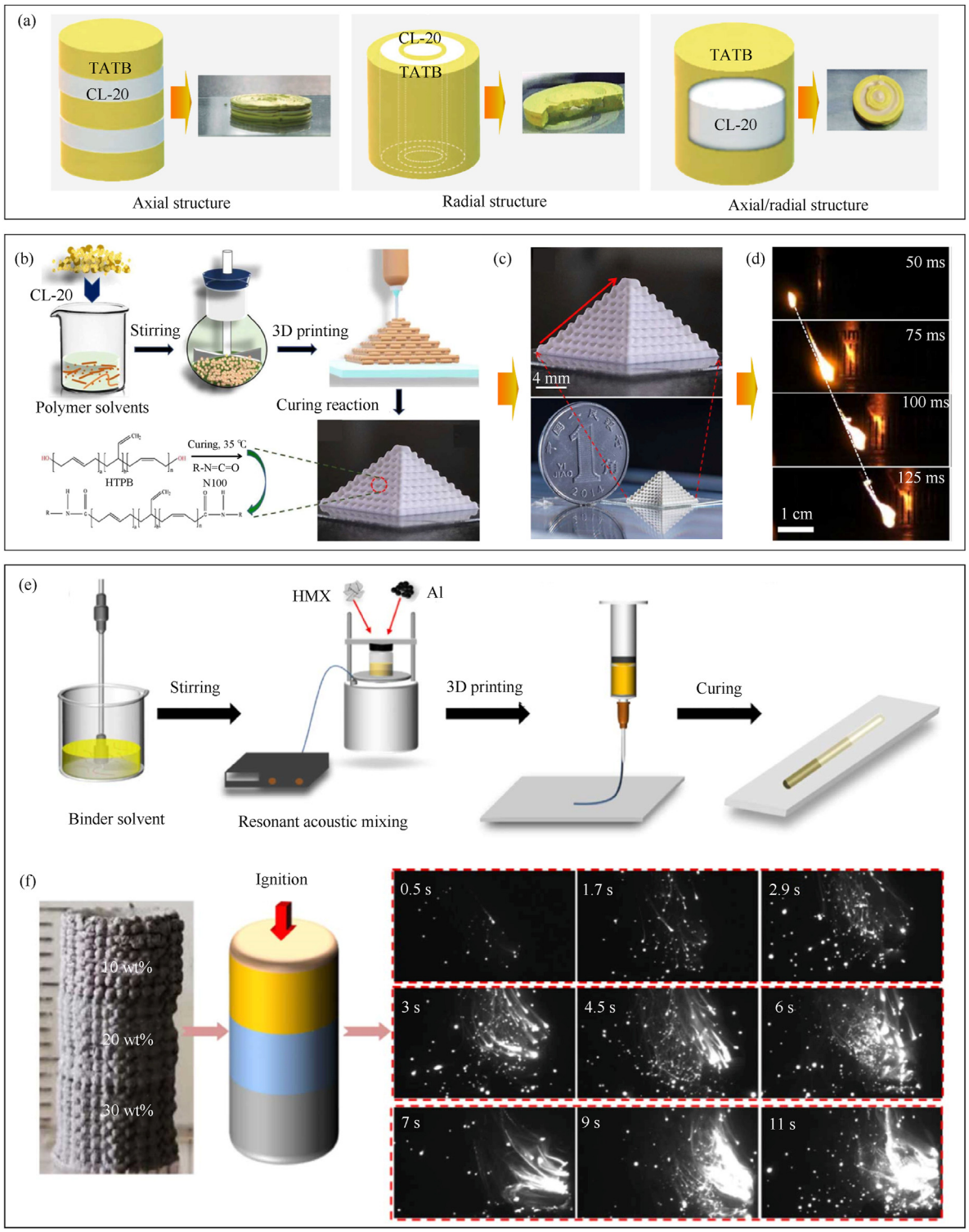

Fig. 25. (a) 3 a.m. TATB/CL-20 composite charge structures (the axial, radial, and axial/radial composite structure). Adapted from Ref. [111]; (b) Schematic illustration of the AM process for CL-20 composites; (c) AM periodic structure; (d) Burning snapshots of AM CL-20 composites (CL-20 85 wt%) with 0.08 mm diameter. The frame rate was 2000 frames per second. Adapted from Ref. [112]; (e) The printing process diagram of gradient structure lines; (f) The combustion process of gradient-structured HMX/Al cylinder. Adapted with permission. Copyright 2021, ELSEVIER publishing [113].

scan of a printed lattice used in Brown's study. Schmalzer et al. [110] use AM technology to intentionally introduce precise internal structures at nearly the mesoscale of explosives, thereby controlling detonation behavior by manipulating complex shock wave interactions. They demonstrated a method to control the directional propagation of reactive flow through the control of the structure of HEs, which implies that AM technology is of great significance for controlling the detonation behavior of HEs.

4.2.2. Gradient structures

Huang et al. [111] determined the best process parameters (binder content of 20%, the printing speed of 3 mm s^{-1}, and the needle diameter of 0.25 mm) for printing the TATB/CL-20 composite structure. Three composite structures are printed (Fig. 25). The safety order of the three structures from high to low is the axial/radial composite structure, the axial structure, and the radial structure. The characteristic drop height of the axial/radial composite structure can reach 72.00 cm. Wang et al. [112] designed and printed a 3D printing ink based on CL-20/HTPB. The schematic illustration of the 3D printing process of CL-20 composites and the printed periodic structure are shown in Figs. 25(b) and 25(c), respectively. The smaller CL-20/HTPB filament has a higher combustion velocity. The burning velocity of the composites with 0.08 mm diameter reached 164.6 mm/s, which validated the potential of AM complex structures with high combustion performance. He et al. [113] designed and prepared the HMX/Al composites with gradient structures using well-dispersed HMX/Al-based inks by AM technology. The preparation process of composites is shown in Fig. 25(e). For gradient-structured HMX/Al, the burning rate could be controlled by varying the component ratio and the burning rate of each component in the gradient structure was higher than that of the ordinary HMX/Al composition. Fig. 25(f) shows the combustion process of gradient structured HMX/Al cylinder. The monitoring results of the pressure output gradient evolution of the laser-ignited gradient structure HMX/Al cylinder demonstrated that the gradient structure can effectively adjust the combustion performance and energy output of HMX/Al. In addition, Wang's team [114] explored the methods of reducing the vulnerability of explosives by adjusting the structure of explosives. The RDX-based aluminum-containing gradient structure explosives were prepared by DIW technology, as shown in Fig. 26(a). The SEM and DSC results demonstrated that the gradient explosive had good compatibility and no obvious void was observed at the filament interface in Figs. 26(d)–26(h), which made the gradient explosive have good thermal stability and inhibited the formation of hot spots. The gradient explosive exhibited significantly higher critical detonation diameter and thickness than a single explosive with the same aluminum content in the whole explosive, nearly two times increase.

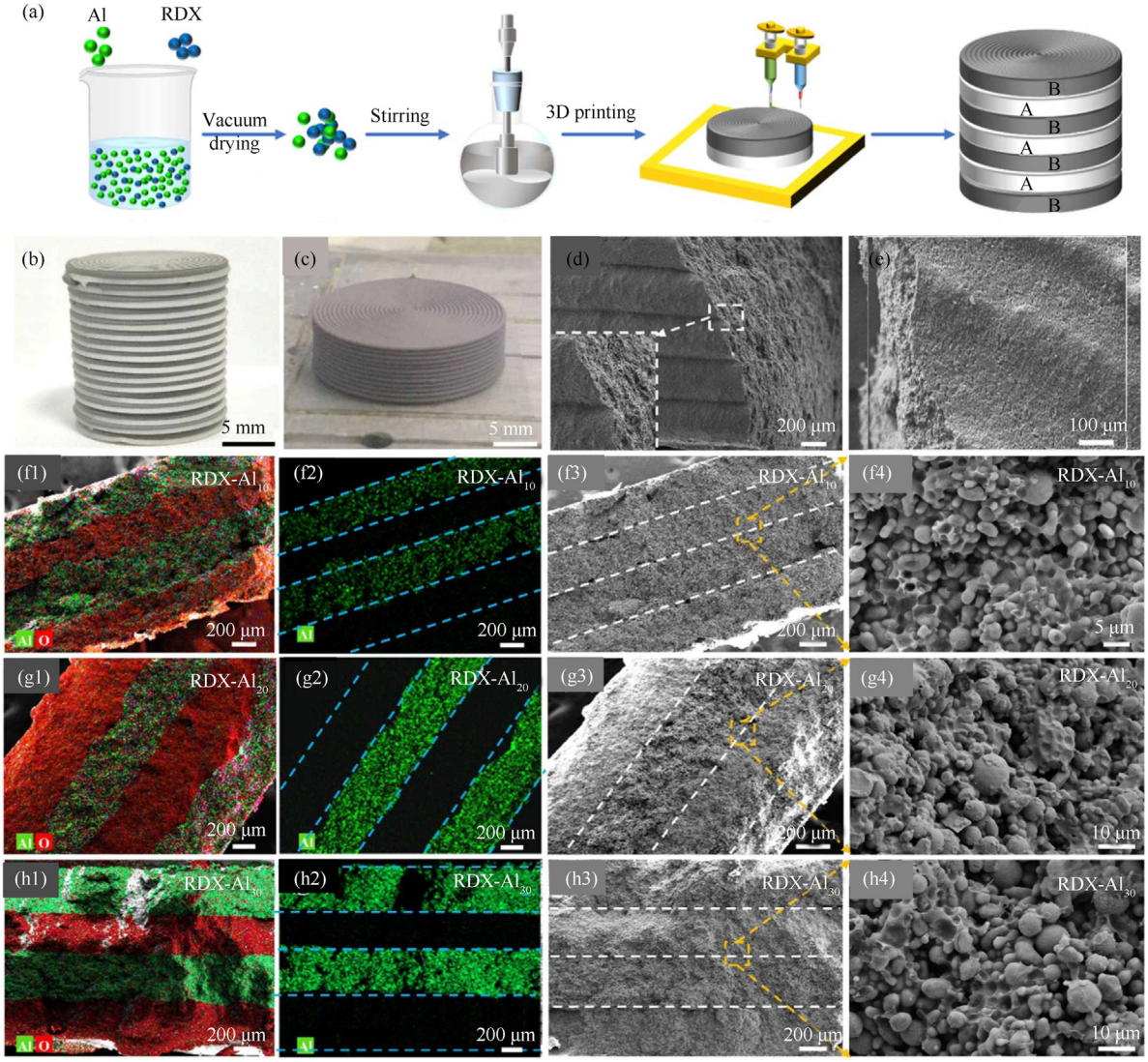

Fig. 26. (a) Preparation process of gradient structured RDX/Al composite; (b) Optical image of RDX-Al_{20} gradient cylinder; (c) Optical image of Al (30 wt%) cylinder; (d–e) SEM images of the side and upper surface of the Al (30 wt%) cylinder; (f–h) SEM and EDS image of RDX-Al_{10}, RDX-Al_{20}, RDX-Al_{30}.
Adapted with permission. Copyright 2021, Springer Publishing [114].

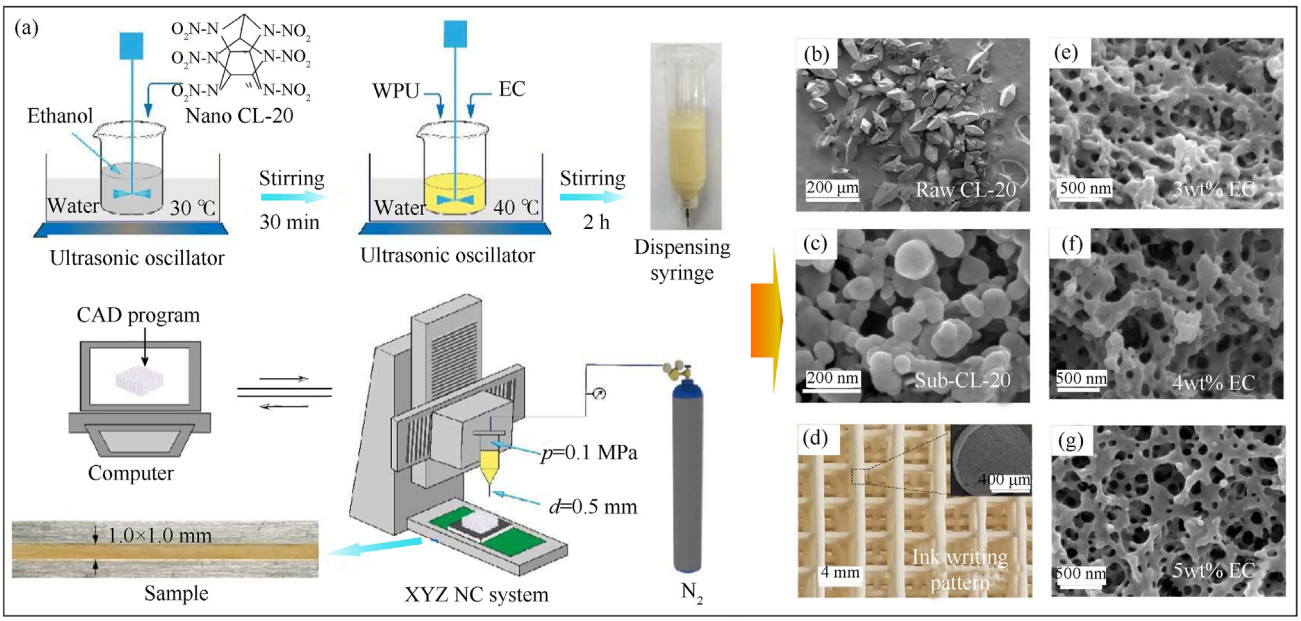

Fig. 27. (a) The schematic for the preparation of the CL-20/WPU/EC ink; SEM images of (b) raw CL-20, (c) sub-CL-20, (d) ink writing pattern, and the corresponding ink samples with different EC contents of 3 wt% (e), 4 wt% (f), and 5 wt% (g).
Adapted with permission. Copyright 2019, ELSEVIER publishing [115].

4.2.3. Honeycomb structures

Ye et al. [115] successfully fabricated AM Honeycombed CL-20 structures with a low critical size of detonation using a micro-flow DIW technology for intelligent weapon systems. The CL-20-based explosive ink by a two-component adhesive system with waterborne polyurethane (WPU) and ethyl cellulose (EC) was prepared, which showed strong shear-thinning behavior that permitted layer-by-layer deposition from a fine nozzle onto a substrate to produce complex shapes, as shown in Fig. 27(a). The shape of the raw CL-20 is spindle-shaped (Fig. 27(b)). After mechanical ball milling, the sub-CL-20 explosives had a nearly spherical shape and smooth surface, whose median size was 140 nm (Fig. 27(c)). Fig. 27(d) shows a 3D periodic structure obtained by writing 10 layers of explosive ink on a substrate, which revealed that the CL-20/WPU/EC ink can be printed in a variety of patterns with high uniformity. As the increase of EC content (Figs. 27(e)–27(g)), the pore size distribution increases.

5. Summary and prospects

Design freedom, parts customization, and manufacturing complex structural components are the significant advantages that AM technology is different from traditional manufacturing, which provides a huge opportunity for improving product performance, exerting multifunction of products, and reducing manufacturing costs. AM technology has made encouraging progress in the past few decades in the fragmentation, shaped charge, and penetrating warheads. In general, AM technology seems to have opened a new door in the warhead field, making the performance of warhead material better and the warhead structure more precise. On the one hand, the material mechanical properties of fragments, liners, and penetrators as well as the combustion performance of explosive

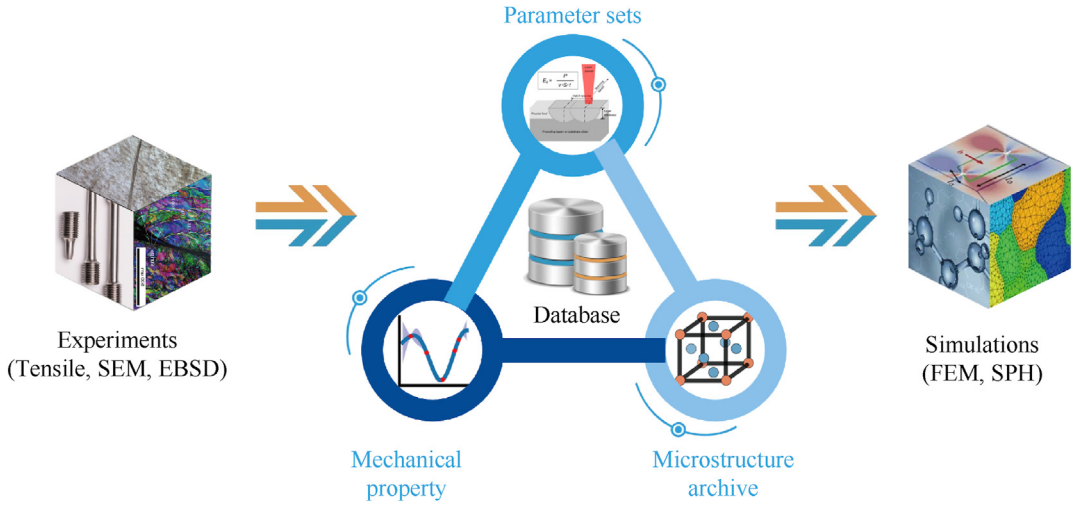

Fig. 28. The concept diagram of the AM materials database.

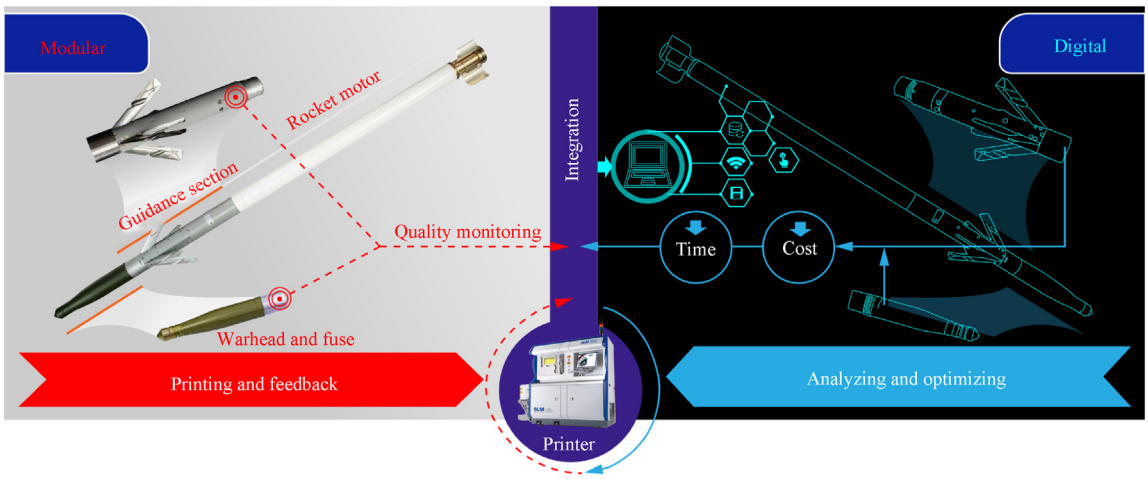

Fig. 29. The concept diagram of digital design and modular manufacturing process of warheads using AM technology. Components such as warheads, fuzes, guidance systems, and rocket engines are digitally designed, and the models are analyzed and optimized through computer platforms. Each module is printed through a printer and the printing information is also fed back to the digital platform in real time. The final missile is obtained after iteration.

compounds manufactured by AM technology have reached or exceeded traditional levels. On the other hand, the special warhead structure and charge structure manufactured by AM technology not only make the damaged elements more powerful but also make the energy more controllable.

In terms of fragmentation warhead, new shell materials, reactive materials, precise shell grooves, and special-shaped warhead structures manufactured by AM technology have greatly changed the damaging effect of the fragmentation warhead by changing the fragment mass, fragment scattering density, fragment energy release, and fragment scattering angle. In terms of the shaped charge warhead, new liner material (CuCrZr and CuSn10) manufactured by AM improves the penetration performance by up to 27% compared with traditional liners. The lightweight liner structures (hollow and honeycomb structures) have also been initially studied in the penetration test, showing certain application potential. In terms of the penetrating warhead, it is of great significance to print new penetrating materials (WHAs, amorphous alloys, and HEAs) with stable performance and good penetrating ability, but related research is still in its infancy. The TO method combined with AM technology can complete the design and manufacturing of a lattice penetrator. Preliminary penetration tests have confirmed the feasibility of the idea, and a reactive material-filled lattice warhead will become a further application direction. In terms of warhead charges, high-energy and insensitive AM explosives are being widely studied. More importantly, AM has completely opened up the development direction of high-precision and energy-customized explosives. By regulating the microstructure of AM explosives (hollow structure, gradient structure, and honeycomb structure), safer explosives are expected to be obtained.

Not limited to these, some bolder outlooks on the application of AM in the warhead field are made, focusing on the following aspects.

(1) Establishment of AM material database

AM materials can be regarded as a new type of materials, whose microstructure and properties are quite different from traditional materials. Existing research mainly focuses on the damage capability of AM warheads, and relevant research on the mechanical properties of warhead materials is scarce. Hence, establishing a complete AM material database covering parameter sets, mechanical properties, and microstructure archives is very important to standardize the application of AM materials. Fig. 28 shows the concept diagram of the AM materials database.

(2) Digital design and modular manufacturing of complex structural warheads

AM technology can realize the digital design of the warhead and quantitatively manufacture a batch of parts with the same property through a set of parameters, which is beneficial to subsequent maintenance and improvement. Moreover, AM makes it easier to achieve modular manufacturing of complex structural warheads. Fig. 29 shows a typical example of using AM technology for digital

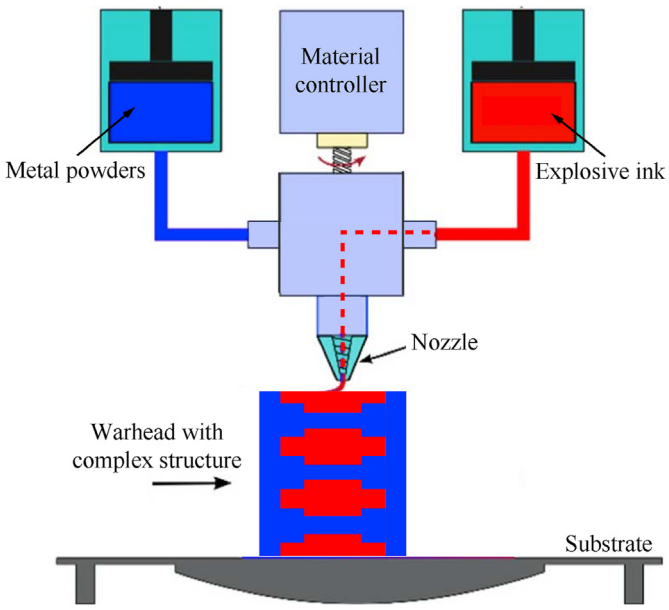

Fig. 30. A possible idea of using AM technology to integrate the manufacturing of warhead shells and charges. By mechanically controlling the delivery of the warhead shell and charging raw materials, the warhead can be manufactured layer by layer according to a predetermined path, greatly shortening the warhead manufacturing cycle.
Adapted from Refs. [116,117].

design and modular manufacturing of warheads, which may completely subvert the traditional warhead manufacturing concept.

(3) Integrated design and manufacturing of warhead and charge

Changing the warhead structure can achieve a controllable output of the damage power, and changing the explosive structure can achieve a controllable release of explosive energy. The design and manufacturing of the integrated warhead and charge structure would achieve precise power release through the dual energy controllability of the AM warhead shell and charge. At present, researchers are working hard to pursue the controllability of the warhead's damage element power and explosive energy. There is no doubt that AM technology is the best choice to combine the two. With the development of hybrid AM, MMAM, and smart AM technology, AM machines that integrate the manufacturing of warheads and charges are expected to be realized. The world's largest multi-material hybrid AM system Kraken is a typical precedent [27]. A possible idea for the integrated AM process of the warhead shell and charge is given in Fig. 30.

Declaration of competing interest

The authors declare that they have no known competing financial interests or personal relationships that could have appeared to influence the work reported in this paper.

Acknowledgments

This work is sponsored by the National Key Research and Development Program of China (Grant No. 2022YFC3320500) and the National Natural Science Foundation of China (Grant Nos. 12372333, 12221002 and 12072037).

References

[1] Zhao S, Yuan S, Cheng C, Shi X, Fu Y. Wang Y.Simulation on forming and penetrating target plate of tungsten alloy pre-fragment warhead. Int J Multiphys 2023;17(2):217–33.
[2] Żochowski P, Warchoł R. Experimental and numerical study on the influence of shaped charge liner cavity filing on jet penetration characteristics in steel targets. Defence Technology 2023;23:60–74.
[3] Tian Q. The development status of selective laser melting technology (SLM). J Phys: Conf Ser 2021;1798:012045.
[4] ISO/ASTM 52900:2021. Additive manufacturing — general principles — fundamentals and vocabulary. 2021.
[5] Durai Murugan P, Vijayananth S, Natarajan MP, Jayabalakrishnan D, Arul K, Jayaseelan V, et al. A current state of metal additive manufacturing methods: a review. Mater Today: Proc 2022;59:1277–83.
[6] Jenzen-Jones NR. Small arms and additive manufacturing:An assessment of 3D-printed firearms, components, and accessories. Behind the Curve: New Technol, New Control Challenges 2015:43–74.
[7] Conant A. Additive manufacturing (AM) and WMD proliferation. In: Kosal ME, editor. Disruptive and game changing technologies in modern warfare: development, use, and proliferation. Cham: Springer International Publishing; 2020. p. 49–69.
[8] Yampolskiy M, Skjellum A, Kretzschmar M, Overfelt RA, Sloan KR, Yasinsac A. Using 3D printers as weapons. Int J Crit Infrastruct Protection 2016;14:58–71.
[9] Xue H, Wang T, Cui X, Wang Y, Huang G. On the ballistic perforation performance of additively manufactured 316 L stainless steel cylindrical projectiles. Int J Impact Eng 2023;178:104625.
[10] Xue H, Wang T, Cui X, Wang Y, Huang G. Ballistic performance of additive manufacturing 316l stainless steel projectiles based on topology optimization method. Defence Technol; 2023. https://doi.org/10.1016/j.dt.2023.06.010.
[11] Seok I, Kilula D, Guo Z. Micro/nanoscale 3-dimensional fabrication using multi-photons polymerization: review. ES Mater Manuf 2023;21:849.
[12] Nagarajan B, Hu Z, Song X, Zhai W, Wei J. Development of micro selective laser melting: the state of the art and future perspectives. Engineering 2019;5:702-720.
[13] Lim JS, Oh WJ, Lee CM, Kim DH. Selection of effective manufacturing conditions for directed energy deposition process using machine learning methods. Sci Rep 2021:11:24169.
[14] Khan S, Joshi K, Deshmukh S. A comprehensive review on effect of printing parameters on mechanical properties of FDM printed parts. Mater Today: Proc 2022;50:2119–27.
[15] Pinargote NWS, Smirnov A, Peretyagin N, Seleznev A, Peretyagin P. Direct ink writing technology (3D printing) of graphene-based ceramic nanocomposites: a review. Nanomaterials 2020;10:1300.
[16] Gülcan O, Günaydın K, Tamer A. The state of the art of material jetting—a critical review. Polymers 2021;13:2829.
[17] Kumaresan R, Samykano M, Kadirgama K, Ramasamy D, Wai KN, Pandey AK. 3D printing technology for thermal application: a brief review. J Adv Res Fluid Mech Thermal Sci 2021;83:84–97.
[18] Mercado Rivera FJ, Rojas Arciniegas AJ. Additive manufacturing methods: techniques, materials, and closed-loop control applications. Int J Adv Manuf Technol 2020;109:17–31.
[19] Sonkamble V, Phafat N. A current review on electron beam assisted additive manufacturing technology: recent trends and advances in materials design. Discov Mech Eng 2023;2:1.
[20] Yang SF, Li CW, Chen AY, Gan B, Gu JF. Microstructure and corrosion resistance of stainless steel manufactured by laser melting deposition. J Manuf Proc 2021;65:418–27.
[21] Tu Y, Arrieta-Escobar JA, Hassan A, Uk uz Zaman, Siadat A, Yang G. Optimizing process parameters of direct ink writing for dimensional accuracy of printed layers. 3D Print Addit. Manuf 2023;10:816–27.
[22] Sireesha M, Lee J, Kranthi Kiran AS, Babu VJ, Kee BBT, Ramakrishna S. A review on additive manufacturing and its way into the oil and gas industry. RSC Adv 2018;8:22460–8.
[23] Rosen DW. Research supporting principles for design for additive manufacturing. Virtual Phys Prototyping 2014;9:225–32.
[24] Hashmi S. Direct rapid tooling. Comprehensive materials processing. 2nd Edition. 2014.
[25] Popov VV, Grilli ML, Koptyug A, Jaworska L, Katz-Demyanetz A, Klobčar D, et al. Powder bed fusion additive manufacturing using critical raw materials: a review. Materials 2021;14:909.
[26] Wang D, Liu L, Deng G, Deng C, Bai Y, Yang Y, et al. Recent progress on additive manufacturing of multi-material structures with laser powder bed fusion. Virtual Phys Prototyping 2022;17:329–65.
[27] Kraken. Project - the future of industrial additive and subtractive manufacturing. https://krakenproject.eu/.
[28] Sher D. 10 top hybrid manufacturing companies. In: VoxelMatters - the heart of additive manufacturing; 2019. https://www.voxelmatters.com/the-top-ten-hybrid-manufacturing-companies/.
[29] AFM. Home | AFM n.d. https://www.afm.es/es/noticias/ibarmia-fabricacion-aditiva-y%EF%BF%BEmecanizado-multitarea-en-una-misma-maquina-en-emo-milano-hall-5.
[30] Rahman MA, Saleh T, Jahan MP, McGarry C, Chaudhari A, Huang R, et al. Review of intelligence for additive and subtractive manufacturing: current status and future prospects. Micromachines 2023;14:508.
[31] Wang Y, Zheng P, Peng T, Yang H, Zou J. Smart additive manufacturing: current artificial intelligence-enabled methods and future perspectives. Sci China Technol Sci 2020;63:1600–11.
[32] Smart Fusion n.d. https://www.eos.info/en/landing-pages/smart-fusion.
[33] Roberts D, Zhang Y, Charit I, Zhang J. A comparative study of microstructure and high-temperature mechanical properties of 15-5 PH stainless steel processed via additive manufacturing and traditional manufacturing. Prog Addit Manuf 2018;3:183–90.
[34] Rafi HK, Starr TL, Stucker BE. A comparison of the tensile, fatigue, and fracture behavior of Ti–6Al–4V and 15-5 PH stainless steel parts made by selective laser melting. Int J Adv Manuf Technol 2013;69:1299–309.
[35] Suryawanshi J, Prashanth KG, Ramamurty U. Mechanical behavior of selective laser melted 316L stainless steel. Mater Sci Eng: A 2017;696:113–21.
[36] Zhou B, Xu P, Li W, Liang Y, Liang Y. Microstructure and anisotropy of the mechanical properties of 316L stainless steel fabricated by selective laser melting. Metals 2021;11:775.
[37] Taban E, Oladimeji Ojo O. Microstructure, mechanical and corrosion behavior of additively manufactured steel: a review (Part 1). Mater Test 2020;62:503–16.
[38] Deng C, Kang J, Feng T, Feng Y, Wang X, Wu P. Study on the selective laser melting of CuSn10 powder. Materials 2018;11:614.
[39] Lin X, Wang H. Application of 3D printing in hypersonic technology. Tactical Missile Technol 2018;105–109.
[40] Helte A, Andersson O, Lundberg P. Deformation, fragmentation and acceleration of a controlled fragmentation charge casing. Defence Technology 2019;15:786–95.
[41] Wang X, Kong X, Zheng C, Wu W. Effect of initiation manners on the scattering characteristics of semi-preformed fragment warhead. Defence Technology 2018;14:578–84.
[42] Zhang F, Gauthier M, Cojocaru CV. Dynamic fragmentation and blast from a reactive Material Solid. Propell, Explos, Pyrotech 2017;42:1072–8.
[43] Tang L, Wang H, Lu G, Zhang H, Ge C. Mesoscale study on the shock response and initiation behavior of Al-PTFE granular composites. Mater Des 2021;200:109446.
[44] Hooper JP. Impact fragmentation of aluminum reactive materials. J Appl Phys 2012;112:043508.

[45] Wang S, Kline J, Miles B, Hooper JP. Reactive fragment materials made from an aluminum–silicon eutectic powder. J Appl Phys 2020;128:065903.
[46] Amott R, Harris EJ, Winter RE, Stirk SM, Chapman DJ, Eakins DE. The fracture and fragmentation behaviour of additively manufactured stainless steel 316L. Florida, USA: Tampa Bay; 2017. p. 100002. https://doi.org/10.1063/1.4971627.
[47] LeSieur AR, Lingenfelter AJ, Guildenbecher DR, Reu PL, Marinis RT, Ball JP. In: Fragmentation properties of explosively driven additively manufactured metals. AIAA scitech 2019 forum. San Diego, California: American Institute of Aeronautics and Astronautics; 2019. https://doi.org/10.2514/6.2019-0776.
[48] Callahan M, Sun D, Linne MA, Wu AS, Campbell GH, Friedman B, et al. Explosive fragmentation of additively manufactured stainless steel. J Appl Phys 2023;134:155105.
[49] Gousman K, Weelden SV, Rosenberger B. Warhead with integral, direct-manufactured features. US20050235862A1; 2005.
[50] Li H, Li G, Chen J, Yuan S, Zhong T, Liu F. Fragment distribution of high-energy-beam controlled fragmentation simulation shell. Weapon Materials Science and Engineering 2009;32:81–4.
[51] Villano D, Galliccia F. Innovative technologies for controlled fragmentation warheads. J Appl Mech 2013;80:031704.
[52] Lu S, Dong S, Wang G, Zhao J, Wang X, Yang D. Performances analysis of precontrol fragment bullet by laser remelting. Sci Technol Eng 2014;14:215–8.
[53] Liu G. Study on the formation and killing power of shell fragment in laser processing. Master. Nanjing University of Science and Technology; 2015.
[54] Guo M. Study on pre-controlled fragmentation of SLM processing. Master. Nanjing University of Science and Technology; 2018.
[55] Rehnberg L, Persson W. Controlled fragmentation of metallic warheads technology development of fragmenting warheads. Karlstad University; 2022.
[56] Yu Zhitong. Study on fragment velocity measurement technology of pre-fabricated fragment warhead. In: 2018 3rd international conference on materials science, machinery and energy engineering (MSMEE 2018). Clausius Scientific Press; 2018.
[57] Xue H, Wang T, Huang G, Cui X, Han H. Ballistic performance of additively manufactured 316L stainless steel SphericalFragments. Acta Armamentarii 2024;45:395–406.
[58] Lewis MK. Developing and testing sintered and polymer-infused 3d-printed aluminum reactive materials. Master. Naval Postgraduate School; 2018.
[59] Ziaee M, Crane NB. Binder jetting: a review of process, materials, and methods. Addit Manuf 2019;28:781–801.
[60] Mulligan P, Johnson C, Ho J, Lough C, Kinzel E. 3D printed conical shaped charge performance 2019 15th hypervelocity impact Symposium. Destin, FL, USA: American Society of Mechanical Engineers; 2019. https://doi.org/10.1115/HVIS2019-110. V001T03A008.
[61] Agu HO, Hameed A, Appleby-Thomas GJ. Comparison of the microstructure of machined and laser sintered shaped charge liner in the hydrodynamic regime. J Dyn Behav Mater 2019;5:484–94.
[62] Ho J, Lough C, Mulligan PR, Kinzel EC, Johnson CE. Additive manufacturing of liners for shaped charges. Austin 2018:479–87.
[63] Liu J, Li W, Zhang Q, Song P, Huang S, Guo X. SLM printing and power test of 316L stainless steel paint cover. J Ordnance Equip Eng 2020;41:5–8.
[64] Song P, Li W-B, Zhang Q, Zheng Y, Huang S-Y, Guo X-J, et al. Experimental research on shell-liner integrated circumferential MEFP warhead based on additive manufacturing. Chin J Explos Propell 2021;44:219–24.
[65] Guo X, Huang S, Song P, Li Y, Liu J, Guo M. Additive manufacturing of copper alloy and its application in Munroe effects. Aopc 2020: advanced laser technology and application. vol. 11562, SPIE 2020:194–198. https://doi.org/10.1117/12.2580011.
[66] Sun S, Jiang J, Wang S, Men J, Li M, Wang Y. Comparison of shaped charge jet performance generated by machined and additively manufactured CuSn10 liners. Materials 2021;14:7149.
[67] Talignani A, Seede R, Whitt A, Zheng S, Ye J, Karaman I, et al. A review on additive manufacturing of refractory tungsten and tungsten alloys. Addit Manuf 2022;58:103009.
[68] Wei C, Ye H, Zhao Z, Tang J, Shen X, Le G, et al. Microstructure and fracture behavior of 90W-7Ni-3Fe alloy fabricated by laser directed energy deposition. J Alloys Compounds 2021;865:158975.
[69] Zhou S, Wang L, Liang Y-J, Zhu Y, Jian R, Wang B, et al. A strategy to achieve high-strength WNiFe composite-like alloys with low W content by laser melting deposition. Mater Des 2020;190:108554.
[70] Li C, Wang Y, Ma S, Yang X, Li J, Zhou Y, et al. Densification, microstructural evolutions of 90W-7Ni-3Fe tungsten heavy alloys during laser melting deposition process. Int J Refractory Metals Hard Mater 2020;91:105254.
[71] Wang YP, Ma SY, Yang XS, Zhou YZ, Liu X, Li JF, et al. Microstructure and strengthening mechanisms of 90W–7Ni–3Fe alloys prepared using laser melting deposition. J Alloys Compd 2020;838:155545.
[72] Li J, Wei Z, Zhou B, Wu Y, Chen S-G, Sun Z. Densification, microstructure and properties of 90W-7Ni-3Fe fabricated by selective laser melting. Metals 2019;9:884.
[73] Chen H, Zi X, Han Y, Dong J, Liu S, Chen C. Microstructure and mechanical properties of additive manufactured W-Ni-Fe-Co composite produced by selective laser melting. Int J Refract Metals Hard Mater 2020;86:105111.
[74] Bruck HA, Christman T, Rosakis AJ, Johnson WL. Quasi-static constitutive behavior of Zr41.25Ti13.75Ni10Cu12.5Be22.5 bulk amorphous alloys. Scripta Metall Mater 1994;30:429–34.
[75] Bruck HA, Rosakis AJ, Johnson WL. The dynamic compressive behavior of beryllium bearing bulk metallic glasses. J Mater Res 1996;11:503–11.
[76] Liu XF, Tian ZL, Zhang XF, Chen HH, Liu TW, Chen Y, et al. "Self-sharpening" tungsten high-entropy alloy. Acta Mater 2020;186:257–66.
[77] Pauly S, Schricker C, Scudino S, Deng L, Kühn U. Processing a glass-forming Zr-based alloy by selective laser melting. Mater Des 2017;135:133–41.
[78] Żrodowski Ł, Wysocki B, Wróblewski R, Kurzydłowski KJ, Święszkowski W. The novel scanning strategy for fabrication metallic glasses by selective laser melting. 2016. Berlin.
[79] Yeh JW, Chen SK, Lin SJ, Gan JY, Chin TS, Shun TT, et al. Nanostructured high-entropy alloys with multiple principal elements: novel alloy design concepts and outcomes. Adv Eng Mater 2004;6:299–303.
[80] Song WL, Ma Q, Zeng Q, Zhu S, Sui M, Cao T, et al. Experimental and numerical study on the dynamic shear banding mechanism of HfNbZrTi high entropy alloy. Sci China-technological Sci 2022;65:1808–18.
[81] Chen H, Zhang X, Dai L, Liu C, Xiong W, Tan M. Experimental study on WFeNiMo high-entropy alloy projectile penetrating semi-infinite steel target. Defence Technology 2022;18:1470–82.
[82] Huang A, Fensin S, Meyers MA. Strain-rate effects and dynamic behavior of high entropy alloys. J Mater Res Technol 2023;22:307–47.
[83] Chadha K, Tian Y, Spray J, Aranas C. Effect of annealing heat treatment on the microstructural evolution and mechanical properties of hot isostatic pressed 316L stainless steel fabricated by laser powder bed fusion. Metals 2020;10:753.
[84] Zhang H, Pan Y, He YZ. Synthesis and characterization of FeCoNiCrCu high-entropy alloy coating by laser cladding. Mater Des 2011;32:1910–5.
[85] Brif Y, Thomas M, Todd I. The use of high-entropy alloys in additive manufacturing. Scripta Mater 2015;99:93–6.
[86] Kuzminova Y, Firsov D, Dudin A, Sergeev S, Zhilyaev A, Dyakov A, et al. The effect of the parameters of the powder bed fusion process on the microstructure and mechanical properties of CrFeCoNi medium-entropy alloys. Intermetallics 2020;116:106651.
[87] Richards H, Liu D. Topology optimization of additively-manufactured, lattice-reinforced penetrative warheads. In: 56th AIAA/ASCE/AHS/ASC structures, structural dynamics, and materials conference. Kissimmee, Florida: American Institute of Aeronautics and Astronautics; 2015.
[88] Provchy ZA, Palazotto AN, Flater PJ. Topology optimization for projectile design. J Dyna Behav Mater 2018;4:129–37.
[89] Jing C-C. Research on topology optimization design method of lattice structure based on selective laser melting technology. Master. Beijing institute of technology; 2017.
[90] Graves WT, Liu D, Palazotto AN. Topology optimization of a penetrating warhead. In: 57th AIAA/ASCE/AHS/ASC structures, structural dynamics, and materials conference. San Diego, California, USA: American Institute of Aeronautics and Astronautics; 2016.
[91] Jr Graves WT, Liu D, Palazotto AN. Impact of an additively manufactured projectile. J Dyn Behav Mater 2017;3:362–76.
[92] Provchy ZA, Palazotto AN. Additively manufactured penetrators. In: 58th AIAA/ASCE/AHS/ASC structures, structural dynamics, and materials conference. Grapevine, Texas: American Institute of Aeronautics and Astronautics; 2017.
[93] Patel A, Palazotto AN. Investigation of hybrid material projectile impact against concrete targets. In: 2018 AIAA/ASCE/AHS/ASC structures, structural dynamics, and materials conference. Kissimmee, Florida: American Institute of Aeronautics and Astronautics; 2018.
[94] Patel AA, Palazotto AN. Design methodology for topology optimization of dynamically loaded structure. J Dyn Behav Mater 2019;5:59–64.
[95] Beard A, Palazotto AN. Alternative materials for high-speed projectile outer casing. In: AIAA scitech 2020 forum. Orlando, FL: American Institute of Aeronautics and Astronautics; 2020.
[96] Al-Ketan O, Rowshan R, Abu Al-Rub RK. Topology-mechanical property relationship of 3D printed strut, skeletal, and sheet based periodic metallic cellular materials. Addit Manuf 2018;19:167–83.
[97] Limido J, Deconinck P, Beaucamp A, Paintendre F, Hereil P-L. Additively manufactured penetrating warheads. EPJ Web Conf 2018;183:04007.
[98] Kim S, Kim S, Kim T, Choi S, Lee TH, Park JS, et al. Topology optimization of reactive material structures for penetrative projectiles. Defence Technology 2022;18:1205–18.
[99] Xiao L, Wang Q, Li W, Liu Q, Hao G, Gao X, et al. Preparation and performances of nano-HMX and TNT melt-cast explosives based on 3D printing technology. Acta Armamentarii 2018;39:1291–8.
[100] Zong H, Guo C, Wang Z, Guo R, Zhou H, Hao G, et al. Preparation of TNT/HMX-based melt-cast explosives with enhanced mechanical performance by fused deposition modeling (FDM). J Energ Mater 2022:1–19.
[101] Zong H, Cong Q, Zhang T, Hao Y, Xiao L, Hao G, et al. Simulation of printer nozzle for 3D printing TNT/HMX based melt-cast explosive. Int J Adv Manuf Technol 2022;119:3105–17.
[102] Ruz-Nuglo Fidel D, Groven Lori J, Puszynski Jan A. Additive manufacturing for energetic components and materials. 2014:894.
[103] Zhang L, Zhang F, Wang Y, Han R, Yang L. Preparation and characterization of direct write explosive ink based on CL-20. J Phys: Conf Ser 2019;1209:012016.
[104] Kong S, Liao D, Jia Y, An C, Li C, Ye B, et al. Performances and direct writing of CL-20 based ultraviolet curing explosive ink. Defence Technology 2022;18:

140–7.
[105] Wang J, Xu C, An C, Song C, Liu B, Wu B, et al. Preparation and properties of CL-20 based composite by direct ink writing. Propell, Explos, Pyrotech 2017;42:1139–42.
[106] Li Q, An C, Han X, Xu C, Song C, Ye B, et al. CL-20 based explosive ink of emulsion binder system for direct ink writing. Propell, Explos, Pyrotech 2018;43:533–7.
[107] Xu C, An C, He Y, Zhang Y, Li Q, Wang J. Direct ink writing of DNTF based composite with high performance. Propell, Explos, Pyrotech 2018;43:754–8.
[108] Laboratory LAN. Explosiv3Design | discover Los Alamos national laboratory. Los Alamos National Laboratory. https://discover.lanl.gov/publications/1663/2016-march/explosiv3-design/.
[109] Brown CB, Mueller AH, Sridhar S, Lichthardt JP, Schmalzer AM, Tappan BC, et al. Switchable explosives: performance tuning of fluid-activated high explosive architectures. Phys Rev Lett 2023;130:116105.
[110] Schmalzer A, Tappan B, Bowden P, Manner V, Clements B, Menikoff R, et al. Controlled detonation dynamics in additively manufactured high explosives. APS Shock Compression of Condensed Matter Meeting; 2017. p. Y2.002.
[111] Huang J, Wang J, Mao Y, Xu R, Zeng G, Yang Z, et al. Preparation of CL-20/TATB composite charge structure by 3D printing technology. Chin J Energ Mater (Hanneng Cailiao) 2019;27:931–5.
[112] Dunju W, Changping G, Ruihao W, Baohui Z, Bing G, Fude N. Additive manufacturing and combustion performance of CL-20 composites. J Mater Sci 2020;55:2836–45.
[113] He Q, Wang J, Mao Y, Yin H, Cao W, Nie F. Fabrication of gradient structured HMX/Al and its combustion performance. Combust Flame 2021;226:222–8.
[114] Zhou X, Mao Y, Zheng D, Zhong L, Wang R, Gao B, et al. 3D printing of RDX-based aluminized high explosives with gradient structure, significantly altering the critical dimensions. J Mater Sci 2021;56:9171–82.
[115] Ye B, Song C, Huang H, Li Q, An C, Wang J. Direct ink writing of 3D-Honeycombed CL-20 structures with low critical size. Defence Technology 2020;16:588–95.
[116] Nazir A, Gokcekaya O, Md Masum Billah K, Ertugrul O, Jiang J, Sun J, et al. Multi-material additive manufacturing: a systematic review of design, properties, applications, challenges, and 3D printing of materials and cellular metamaterials. Mater Des 2023;226:111661.
[117] Hasanov S, Alkunte S, Rajeshirke M, Gupta A, Huseynov O, Fidan I, et al. Review on additive manufacturing of multi-material parts: progress and challenges. J Manuf Mater Process 2021;6:4.